Published online 6 December 2016 *Nucleic Acids Research, 2017, Vol. 45, No. 3* ***1371–1391***
doi: 10.1093/nar/gkw1234

Sinorhizobium meliloti YbeY is an endoribonuclease with unprecedented catalytic features, acting as silencing enzyme in riboregulation

Margarida Saramago[1,†], Alexandra Peregrina[2,†], Marta Robledo[2,†], Rute G. Matos[1], Rolf Hilker[3], Javier Serrania[3], Anke Becker[3], Cecilia M. Arraiano[1] and José I. Jiménez-Zurdo[2,*]

[1]Instituto de Tecnologia Química e Biológica António Xavier, Universidade Nova de Lisboa, Avenida da República, 2780-157 Oeiras, Portugal, [2]Grupo de Ecología Genética de la Rizosfera, Estación Experimental del Zaidín, Consejo Superior de Investigaciones Científicas (CSIC), 18008 Granada, Spain and [3]LOEWE Center for Synthetic Microbiology and Faculty of Biology, Philipps-University Marburg, 35043 Marburg, Germany

Received April 01, 2016; Revised November 22, 2016; Editorial Decision November 24, 2016; Accepted November 24, 2016

ABSTRACT

Structural and biochemical features suggest that the almost ubiquitous bacterial YbeY protein may serve catalytic and/or Hfq-like protective functions central to small RNA (sRNA)-mediated regulation and RNA metabolism. We have biochemically and genetically characterized the YbeY ortholog of the legume symbiont *Sinorhizobium meliloti* (*Sm*YbeY). Co-immunoprecipitation (CoIP) with a FLAG-tagged *Sm*YbeY yielded a poor enrichment in RNA species, compared to Hfq CoIP-RNA uncovered previously by a similar experimental setup. Purified *Sm*YbeY behaved as a monomer that indistinctly cleaved single- and double-stranded RNA substrates, a unique ability among bacterial endoribonucleases. *Sm*YbeY-mediated catalysis was supported by the divalent metal ions Mg^{2+}, Mn^{2+} and Ca^{2+}, which influenced in a different manner cleavage efficiency and reactivity patterns, with Ca^{2+} specifically blocking activity on double-stranded and some structured RNA molecules. *Sm*YbeY loss-of-function compromised expression of core energy and RNA metabolism genes, whilst promoting accumulation of motility, late symbiotic and transport mRNAs. Some of the latter transcripts are known Hfq-binding sRNA targets and might be *Sm*YbeY substrates. Genetic reporter and *in vitro* assays confirmed that *Sm*YbeY is required for sRNA-mediated down-regulation of the amino acid ABC transporter *prbA* mRNA. We have thus discovered a bacterial endoribonuclease with unprecedented catalytic features, acting also as gene silencing enzyme.

INTRODUCTION

The *ybeY* gene is almost ubiquitous in bacteria and has been included in the minimal prokaryotic genome set (1–3). These evidences support a rather fundamental physiological role of its protein product. Accordingly, YbeY loss-of-function is lethal in some bacterial species and in others can result in pleiotropic changes (3–8). Structural studies of YbeY orthologs uncovered a conserved three histidine H(X)3H(X)4DH motif shared by metallo-hydrolases and global similarity to the MID domain of eukaryotic AGO proteins involved in small RNA-directed gene silencing (9–12). These features suggest that YbeY could serve catalytic and/or RNA-binding/chaperone functions in bacteria. However, the biochemical activity of this protein has remained elusive until recently.

Escherichia coli YbeY (from here on *Eco*YbeY) has been shown to be required for efficient translation, optimal activity of the 30S ribosomal subunit and accurate ribosome assembly, particularly upon a temperature upshift (5,13–15). The severe defects of *Eco*YbeY deletion mutants in ribosome biogenesis have been mainly attributed to a failure in *rrn* transcription anti-termination and abnormal maturation of the rRNA precursors, which together result in accumulation of misprocessed 16S, 23S and 5S rRNA species (5,13,16). Similar effects on rRNA maturation have been also described for YbeY orthologs of the human pathogens *Yersinia enterocolitica* and *Vibrio cholerae* (7,8). Supporting these observations it has been also reported that the purified *Eco*YbeY acts as a single strand-specific metallo-endoribonuclease (13). The H114 residue within the histi-

*To whom correspondence should be addressed. Tel: +34 958181600; Fax: +34 958181609; Email: jijz@eez.csic.es
†These authors contributed equally to the work as the first authors.

dine triad involved in metal binding and the arginine R59 integrating another conserved cluster of amino acids are required for *Eco*YbeY activity *in vivo* and *in vitro* (5,12,13). Processing of the rRNA precursors to their functional mature forms *in vivo* involves the concerted activity of additional RNases, including RNase III, RNase R, RNase E, RNase G and PNPase (5,13,17). Indeed, YbeY and RNase R are major components of a remarkable late-ribosome quality control system, particularly important for stress survival, which mediates removal of assembled 70S ribosomes specifically containing defective 30S subunits (13).

Structural modeling of the YbeY protein encoded by the nitrogen-fixing symbiotic bacterium *Sinorhizobium meliloti* evidenced a positively charged cavity resembling the AGO MID domain that anchors si/miRNAs to the RNA-induced silencing complex (10,18,19). In bacteria, a large fraction of the known small non-coding RNAs (sRNAs) regulates translation and/or stability of *trans*-encoded target mRNAs (20). To date, the chaperone activity assisting *trans*-sRNA function has been almost exclusively attributed to the widespread bacterial RNA-binding protein Hfq (21,22). However, nearly half of the sequenced bacterial genomes do not encode a recognizable Hfq homolog and several well-characterized *trans*-sRNAs have been shown to be Hfq-independent (23–25). For example, in *S. meliloti* only 14% of the annotated *trans*-acting sRNAs bind to Hfq (26). These observations suggest that other proteins may assist sRNA-mediated post-transcriptional control of gene expression. YbeY has been proposed to fulfil this important role since: (i) lack or depletion of YbeY results in differential accumulation of subsets of sRNAs and their predicted mRNA targets in *E. coli*, *S. meliloti* and *V. cholerae* (8,10,27) and (ii) YbeY and Hfq similarly influence *S. meliloti* sensitivity to a number of stress agents (e.g. paraquat, SDS, ethanol, NaCl or heat) and the symbiotic interaction with its legume host, alfalfa (3,10,28). However, these studies did not provide data supporting an active role of YbeY in the sRNA–mRNA interplay.

In this work, we have purified and characterized *S. meliloti* YbeY (from here on *Sm*YbeY) regarding its RNA-binding ability and biochemical activity. Furthermore, we have also investigated the influence of *Sm*YbeY loss-of-function in the *S. meliloti* transcriptome. Our results show that this protein acts as a metal-dependent single and double-strand endoribonuclease rather than as Hfq-like RNA chaperone. *Sm*YbeY activity profoundly impacts on conserved fundamental chromosomally-encoded functions as well as on certain acquired plasmid-encoded *S. meliloti* pathways. We also provide evidences of the involvement of *Sm*YbeY in the Hfq-dependent riboregulation of amino acid uptake.

MATERIALS AND METHODS

Bacterial strains, plasmids, culture conditions and oligonucleotides

Bacterial strains and plasmids used in this work along with their relevant characteristics are listed in Supplementary Table S1. Oligonucleotide sequences are provided in Supplementary Table S2. *E. coli* strains were routinely grown in Luria–Bertani medium (LB) at 37°C and rhizobia in either complex tryptone-yeast (TY) or defined MM media at 30°C (29,30). When required, growth media were supplemented with the appropriate antibiotic(s) at the following final concentrations (μg/ml) unless otherwise stated: streptomycin (Sm) 250, ampicillin (Ap) 200, tetracycline (Tc) 10, erythromycin (Er) 100, gentamicin (Gm) 45 and kanamycin (Km) 50 for *E. coli* and 180 for rhizobia.

For co-immunoprecipitation (CoIP) experiments wild-type and Sm*ybeY*^{FLAG} strains were subjected to five different growth/stress conditions in 50 ml broth. Exponential and stationary cultures were obtained in TY medium upon bacterial growth to OD_{600} 0.6 and 2.8, respectively. Cold and heat shocks were applied to exponentially growing bacteria in TY during 1 h by shifting the temperature to 20°C and 42°C, respectively. The salt shock was imposed during 1 h by addition of 0.4 M NaCl to exponential cultures in MM medium.

Construction of *S. meliloti* mutants and derivative strains

*Sm*YbeY is encoded by the gene annotated as SMc01113 in the genome of the reference Rm1021 strain (31). *S. meliloti* Sm*ΔybeY* and Sm*ybeY*^{FLAG} derivatives were both generated in the ExpR^+ Sm2011 derivative strain Sm2B3001 (32). To create an in-frame deletion of *ybeY*, 938-bp and 921-bp DNA fragments flanking the SMc01113 ORF were PCR amplified from genomic DNA with primer pairs YbeY_F1/YbeY_iR and YbeY_iF/YbeY_R1. Primers YbeY_iR and YbeY_iF carry *Hind*III sites at their 5′-ends. The resulting PCR products were thus restricted with *Hind*III and ligated to each other. The ligation reaction was used as a template for a second PCR with primers YbeY_FS and YbeY_RE that yielded a 1871-bp DNA fragment flanked by *Eco*RI sites and containing the *ybeY* deletion with the junction sequence ATGACGGCGAAGCTTTAA. This fragment was digested with *Eco*RI and inserted into the suicide vector pK18*mobsacB* (33) to yield pK18Δ*ybeY*, which was mobilized to the Sm2B3001 strain by a biparental mating involving *E. coli* S17-1 (34). Recombinants that underwent single and double crossover events were subsequently isolated by Km resistance and counter-selection in 10% sucrose as described in (35). Deletion of *ybeY* in the selected double recombinant was confirmed by PCR with primers YbeY_MutF and YbeY_MutR followed by *Hind*III restriction of the PCR product as well as by full re-sequencing of parent and mutant strain genomes on an Illumina MiSeq System applying a TruSeq, V2 Chip (2 × 250 bp) (Supplementary Figure S1).

Mutant Sm*ΔybeY* was complemented with plasmid pJBYbeY expressing *Sm*YbeY from its own promoter. For that, an 810-bp genomic DNA fragment containing the *Sm*YbeY coding sequence along with 266 nt of its upstream region was PCR-amplified with the primers pair YbeY_PrF/YbeY_PrR. The PCR product was first cloned into the pGEM-T® Easy vector (Promega Corporation), then retrieved by *Hind*III-*Eco*RI restriction and finally inserted into the low copy vector plasmid pJB3Tc19 (36) to generate pJBYbeY, which was conjugated into the Sm*ΔybeY* mutant by biparental mating.

The *loci* encoding the *trans*-sRNAs AbcR1 and AbcR2 were deleted in both the parent Sm2B2001 and the SmΔ*ybeY* strains by allelic replacement mediated by plasmid pK18EryΔR1/2 (37) to generate the double Sm2B2001ΔR1/2 and triple SmΔR1/2Δ*ybeY* mutants.

Tagging of *ybeY* with the FLAG epitope (Sigma-Aldrich) to generate the Sm*ybeY*^{FLAG} strain was done as follows. The full-length *Sm*YbeY coding sequence (devoid of its TAA stop codon) along with 935 nt of its upstream genomic region was amplified by PCR with the pair of primers YbeY_F1/YbeY_XbaI, the latter adding a *Xba*I restriction site to the 3′-end of the fragment. The PCR product was first cloned into pGEM-T® Easy, retrieved as a *Sac*II (genomic site internal to the PCR product)-*Xba*I fragment and finally inserted upstream of the DNA sequence coding for three tandem FLAG epitopes in the previously constructed pKS3xFLAG plasmid (35) to generate pSK5′YbeYFlag. A second 921-bp genomic DNA fragment, starting with the *Sm*YbeY stop codon, was generated by PCR with primers YbeY_iF and YbeY_RK that add *Hind*III and *Kpn*I restriction sites to its 5′ and 3′ ends, respectively. This PCR product was cloned into pGEM-T® Easy, then excised as a *Hind*III-*Kpn*I DNA fragment and inserted immediately downstream of the 3xFLAG DNA sequence in pSK5′YbeYFlag to yield pKSYbeY3xFlag. Finally, a 2372-bp DNA fragment encoding the C-terminal FLAG-tagged *Sm*YbeY was amplified from pKSYbeY3xFlag with the primers pair YbeY_FS/YbeY_RE, then digested with *Eco*RI and inserted into pK18*mobsacB* to generate the suicide plasmid pK18YbeY3xFlag. This plasmid was mobilized to the Sm2B3001 strain by biparental mating for replacement of wild-type *ybeY* by the modified allele. Presence of *ybeY*^{FLAG} in several double recombinants selected as previously described was confirmed by PCR on genomic DNA with primers YbeY_MutF and YbeY_MutR, *Xba*I restriction of the PCR products and Western blot analysis with commercial ANTI-FLAG monoclonal antibodies (Sigma-Aldrich) following a published protocol (35).

All PCR reactions required for cloning were performed with the proofreading Phusion™ High-Fidelity DNA polymerase (Thermo Scientific). Plasmid inserts were always checked by sequencing to confirm the absence of PCR-introduced mutations.

CoIP-RNA preparation, RNAseq and data analysis

Exponential, stationary, cold, heat and salt stressed cultures of both Sm2B3001 (control) and Sm*ybeY*^{FLAG} strains were obtained as described, and 50 ml of each culture were pooled before bacterial lysis by sonication. CoIP–RNA was obtained from both control and Sm*ybeY*^{FLAG} lysates using the ANTI-FLAG M2 affinity gel (Sigma) followed by organic extraction as described (26). This procedure was performed twice and equivalent quantities of CoIP–RNA from each replicate and strain were finally pooled.

Control and Sm*ybeY*^{FLAG} CoIP–RNA pools were further processed by Vertis Biotechnologie AG to generate two strand-specific cDNA libraries as previously described (26). Libraries were sequenced on an Illumina MiHiSeq System applying a TruSeq, V3 Chip (2 × 300 bp).

After sequencing, reads were demultiplexed based on their sequence indices and mapped with Bowtie2 version 2.1.0 (38), using standard parameters after quality trimming, to the *S. meliloti* Rm1021 reference sequence (31). Data visualization and analysis based on an updated version of the *S. meliloti* public GenDB project including annotations of identified sRNAs (39,40) were done with the ReadXplorer software (41). Within ReadXplorer, the Express test and DESeq2 (42) tools were used to identify transcripts differentially represented in Control and Sm*ybeY*^{FLAG} CoIP–RNA.

Overexpression, purification and cross-linking of recombinant *Sm*YbeY and *Sm*YbeY-R69A

The *S. meliloti ybeY* gene was amplified by PCR from genomic DNA of strain Sm2B3001 with Phusion High-Fidelity DNA polymerase using the primers YbeY_F2 and YbeY_R2. The purified 529-bp PCR product was double digested with *Nde*I and *Bam*HI and cloned into the histidine tag-containing pET15b vector (Novagen) to yield pET15b-SmYbeY. The point mutation R69A was introduced into pET15b-SmYbeY by site-directed mutagenesis using primers R69A_F and R69A_R, originating plasmid pET15b-SmR69A. Both constructs were checked by sequencing (STAB Vida, Portugal).

Both plasmids were transformed into *E. coli* BL21(DE3) (Novagen) for the expression of the recombinant proteins. Cells were grown at 37°C to an OD_{600} of 0.5 in 100 ml LB medium supplemented with 100 μg/ml ampicillin. At this point, protein expression was induced by addition of 0.5 mM IPTG and bacteria were grown for a further 4 h. Cells were pelleted by centrifugation and stored at −80°C. The culture pellet was resuspended in 3 ml of Buffer A (10 mM Tris-HCl, 200 mM potassium acetate, 5 mM β-mercaptoethanol, pH 7.5). Cell suspension was lysed using a French Press at 1000 psi in the presence of 0.1 mM PMSF. The crude extract was treated with Benzonase (Sigma) to degrade the nucleic acids and clarified by a 30 min centrifugation at 10 000 *g*. Purification was performed in an ÄKTA FPLC™ system (GE Healthcare). The cleared lysate was subjected to a histidine affinity chromatography in a HisTrap HP column (GE Healthcare) equilibrated in Buffer A. Proteins were eluted by a continuous imidazole gradient up to 500 mM in Buffer A. The fractions containing the purified protein were pooled together, concentrated and buffer exchanged to Buffer B (20 mM Tris-HCl pH7.5) using a HiTrap Desalting column (GE Healthcare). The proteins were then added to a HiTrap Q HP column (GE Healthcare) equilibrated in Buffer B to perform anion exchange. Protein elution was achieved by a continuous NaCl gradient up to 1 M in buffer B. Eluted proteins were concentrated by centrifugation at 4°C with Amicon Ultra Centrifugal Filter Devices of 10 000 MWCO (Millipore), and buffer exchanged to Buffer A. The purity of the proteins was verified in a 15% SDS-PAGE gel followed by BlueSafe staining (Nzytech, Portugal). Proteins were quantified using the Bradford Method and 50% (v/v) glycerol was added to the final fractions prior storage at −20°C. RNase E from *Salmonella enterica* serovar Typhimurium, used as a control in the activity assays, was purified as described (43).

To verify if *Sm*YbeY is able to form oligomers, 0.5 μg of the purified recombinant protein were incubated in a 10 μl cross-linking reaction with 10 mM Hepes pH 7.4, 250 mM NaCl, 0.1 mM EDTA, 0.1 mM DTT and increasing concentrations (1–20 μg) of disuccinimidyl suberate. The reaction was performed at room temperature for 30 min and quenched by adding 1 μl of Tris-HCl 1M pH 7.5 and SDS loading buffer. The samples were boiled during 5 min and then analyzed in a 15% SDS-PAGE gel. RNase III, which is active as a dimer, was used as a positive control.

In vitro production of RNA substrates and *Sm*YbeY activity assays

The single-stranded RNA substrates used in the *in vitro* activity assays were the synthetic 16-mer and 30-mer oligoribonucleotides (Supplementary Table S2), which were labeled at their 5′ end with [γ-^{32}ATP] and T4 Polynucleotide Kinase (Ambion) in a standard reaction. Both RNA molecules were also hybridized to a complementary non-labeled 16-mer oligoribonucleotide added in excess (molar ratio 1:5) in order to obtain a perfect 16-16ds duplex, and a 30–16ds double stranded substrate with a 3′poly(A) tail. The hybridization was performed during 10 min at 80°C followed by 45 min at 37°C.

The R1.1 RNA, the unprocessed 3′ terminus of the 16S rRNA (39-mer), and the complementary 3′ terminus 16S rRNA were generated using a synthetic DNA template (R1.1 REV, 3′ 16S-rRNA Sm (39-mer) REV and 3′ 16S-rRNA Sm complementary, respectively) and a commercial promoter oligonucleotide (T7 FW) (StabVida, Portugal) for *in vitro* transcription, following a previously described method (44). Briefly, the synthetic DNA template (0.5 μM) and the promoter oligonucleotide (0.6 μM) were annealed in 10 mM Tris-HCl pH 8.0 by heating for 5 min at 70°C, followed by 30 min incubation at 37°C. *In vitro* transcription was carried out using the 'Riboprobe *in vitro* Transcription System' (Promega) and T7 RNA polymerase with a molar excess of [^{32}P]-α-UTP over non-radioactive UTP. In order to remove the DNA template, 1 U of DNase (Promega) was added and incubated 30 min at 37°C. RNA transcripts generated from *in vitro* transcription were purified by electrophoresis on an 8.3 M urea/polyacrylamide gel. The gel slice was crushed and the RNA was eluted overnight at room temperature with elution buffer [3 M ammonium acetate pH 5.2, 1 mM EDTA, 2.5% (v/v) phenol pH 4.3]. The RNA was ethanol precipitated, resuspended in RNase free water and quantified using the Biophotometer Plus (Eppendorf). tRNA-Ser, AbcR2, 5′-prbA, *ugpA* and SMa_asRNA_345 RNAs were similarly generated, however, the corresponding DNA templates for *in vitro* transcription were produced by PCR using genomic DNA from *S. meliloti* Rm2011 strain (primer pairs on Supplementary Table S2). The phage T7 RNA polymerase promoter sequence was included in the forward primers. *ybeY* mRNA was generated using pET15b-SmYbeY (Supplementary Table S1) as template for *in vitro* transcription. The phage T7 RNA polymerase promoter sequence is included in the plasmid. In all cases the yield of the labeled substrates (cpm/μl) was determined by scintillation counting.

The activity assays were performed in a final volume of 50 μl containing the activity buffer 25 mM Tris-HCl pH 7.5, 150 mM NaCl or KCl and 10 mM $MgCl_2$, $MnCl_2$ or $CaCl_2$ for *Sm*YbeY or 25 mM Tris-HCl pH 7.5, 5 mM $MgCl_2$, 60 mM KCl, 100 mM NH_4Cl, 0.1 mM DTT and 5% (v/v) glycerol for RNase E and the RNA substrate (concentrations indicated in the figure legends). As a control, an aliquot of each reaction (without the enzyme) was incubated until the end of the assay. The reactions were started by the addition of the enzyme, and further incubated at 37°C in case of *Sm*YbeY. Aliquots of 5 μl were withdrawn at different time-points, and the reactions were stopped by the addition of formamide containing dye supplemented with 10 mM EDTA. Reaction products were resolved in a 7M urea/polyacrylamide gel at different concentrations and visualized by PhosphorImaging (FLA-2000, Fuji, Stamford, CT, USA). Each activity assay was performed at least in triplicate.

Radioactive RNA molecules used as substrates in gel shift assays are described above. Non-radioactive complementary 3′ 16S rRNA was transcribed in the same conditions but using equimolar concentrations of all four ribonucleotides. *In vitro* transcription products were run on a polyacrylamide gel, identified by ethidium bromide staining and the full-length RNA molecules were cut out from the gel. RNA was eluted from the gel slice as described above. The hybridization between labeled and non-labeled substrates was always performed in the Tris component of the activity buffer by incubation for 10 min at 80°C, followed by 45 min at 37°C. A molar excess of the non-labeled substrates were added to the labeled RNA. The molar ratio of unlabeled to labeled substrate molecules was 5:1. The binding reactions were then mixed with loading buffer (48% glycerol, 0.01% bromophenol blue) and electrophoresed on native polyacrylamide gels in 0.5X TBE buffer at 200V in a cold room. Gels were analyzed using PhosphorImaging (FLA-2000, Fuji, Stamford, CT, USA).

Microarray-based transcriptomics

Total RNA was obtained from four independent exponential (OD_{600} 0.5) and stationary (OD_{600} 2.5) cultures of each strain, i.e. Sm2B3001 and the Sm*Δybe Y* mutant (eight preparations per strain), with the RNeasy Mini Kit (Qiagen). cDNA synthesis, Cy3- and Cy5-labeling, hybridization to Sm14kOLI microarrays, image acquisition and data analysis were performed as previously described (45). The Sm14kOLI microarray (ArrayExpress Accession No. A-MEXP-1760) carries 50mer to 70mer oligonucleotide probes directed against coding regions and both strands of the intergenic regions (*Sinorhizobium meliloti* 1021 Sm14kOLI) (46). Probes in intergenic regions were separated by ∼50 to 100 nt. Normalization and t-statistics were carried out using the EMMA 2.8.2 microarray data analysis software (47). Genes and 5′-/3′-UTRs with *P*-value ≤0.05 and M ≥1.0 or ≤−1.0 were included in the analysis. The M value represents the log2 ratio between both channels. Transcriptome data are available at ArrayExpress under accession number E-MTAB-5233. Functional categories of the differentially expressed genes were established according to the *S. meliloti* Rm1021 genome se-

quence annotation (31) and the KEGG database (http://www.genome.jp/kegg/).

Fluorescence reporter assays

Influence of *Sm*YbeY and AbcR2 sRNA on the post-transcriptional regulation of the *prbA* mRNA was further investigated by a double-plasmid reporter assay as described (26,48). Briefly, the reporter plasmid pR*prbA::egfp* (26), which constitutively expresses a translational fusion of the 5′ region of *prbA* mRNA (i.e. 211 nt spanning from its native transcription start site to the 18th codon) to eGFP, or the control pBBsyn-eGFP (48) were first transferred to the Sm2B3001 strain and its mutant derivative SmΔ*ybeY*. A second series of reporter strains was generated by conjugation of pR*prbA::egfp* into Sm2B2001ΔR1/2 and SmΔR1/2Δ*ybeY* harboring pSRK-R2, expressing AbcR2 constitutively, or the empty control plasmid pSRK_C (37). pSRK-R2b, which expresses an AbcR2 variant mutated for base-pairing with *prbA*, was generated by overlapping PCR with primers PCR3_F and PCR1_R of DNA fragments amplified from pSRK-R2 with the primer pairs PCR3_F/AbcR2_R and AbcR2b_F/PCR1_R, followed by *Bam*HI/*Sac*I restriction of the full-length product and insertion into pSRK-C. eGFP-mediated fluorescence in normalized exponential cultures of three double transconjugants for each plasmid combination was measured in the Infinite M200 Pro microplate reader (Tecan) as described (26).

RESULTS

Genome-wide profiling of RNAs bound to *Sm*YbeY

As global approach to explore the proficiency of *Sm*YbeY to bind RNA we profiled the RNA species co-immunoprecipitated (CoIP-RNA) with a C-terminal FLAG-tagged variant of the protein (*Sm*YbeY^{FLAG}) expressed from the chromosome of the Sm2B3001 strain. Unlike the *ybeY* deletion mutant (SmΔ*ybeY*), the Sm*ybeY*^{FLAG} derivative strain exhibited wild-type growth in complete TY and minimal MM media, indicating that tagging did not compromise *Sm*YbeY function (Supplementary Figure S2). The untagged wild-type strain was used as control to assess unspecific RNA recovery. Control and *Sm*YbeY^{FLAG} CoIP–RNA, both obtained from bacterial pools representing five different growth conditions (i.e. exponential and stationary cultures and salt, heat and cold shocks), served as the templates to generate strand-specific cDNA libraries that were subjected to paired-end sequencing on an Illumina platform. Before organic extraction of the CoIP–RNA, the presence of *Sm*YbeY^{FLAG} in the RNA–protein complexes was verified by Western-blot (Supplementary Figure S3). RNaseq delivered an average of 4 200 000 reads per library of which 1 150 974 (C-wt library) and 1 406 485 (*Sm*YbeY^{FLAG}-derived library) mapped to unique locations within the reference *S. meliloti* Rm1021 genome. We then applied the DESeq2 and Express tests, both implemented in the ReadXplorer software (41), to the sets of uniquely mapped reads in order to identify transcripts differentially represented in both libraries. Transcripts covered by a minimum of 30 reads and enriched at least 2-fold in the *Sm*YbeY^{FLAG} library with respect to the control were scored as *Sm*YbeY-bound (i.e. *Sm*YbeY RNAs).

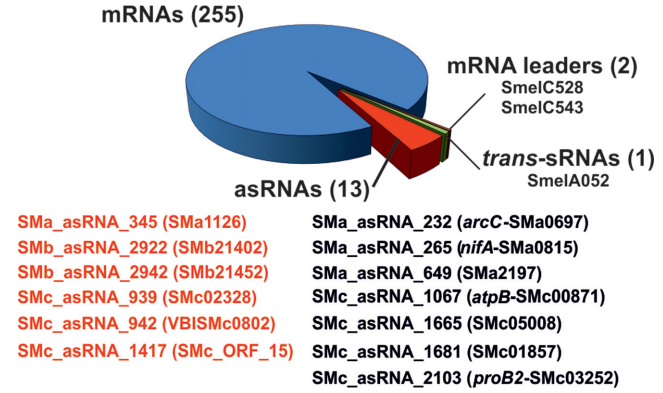

Figure 1. Identification of *Sm*YbeY-binding transcripts. The diagram shows the number of different RNA species, i.e. mRNAs, asRNAs, mRNA leaders and *trans*-sRNAs, enriched ≥2-fold in *Sm*YbeY^{FLAG} CoIP–RNA with respect to the control. The identified asRNA/mRNA pairs are in red color.

The combination of both tests rendered a catalog of 271 *Sm*YbeY RNAs (Supplementary Table S3). Of those, 255 (94%) derived from mRNAs, 13 (4.8%) were annotated antisense sRNAs (asRNAs) and 3 (1.2%) represent other sRNAs (2 mRNA leaders and 1 *trans*-sRNA) (Figure 1). It is worth noting that the mRNA partners of 6 out of the 13 *Sm*YbeY asRNAs were catalogued as *Sm*YbeY-bound. This observation hints at certain affinity of *Sm*YbeY for asRNA–mRNA duplexes.

If we compare the *Sm*YbeY and Hfq CoIP–RNAs, the latter obtained using a similar experimental setup in the same culture conditions (26), we conclude that *Sm*YbeY does not have Hfq-like RNA chaperone features.

*Sm*YbeY is a metal-dependent single- and double-strand endoribonuclease

We have purified *Sm*YbeY and performed the first characterization of its biochemical activity. Cross-linking of the recombinant protein with increasing amounts of disuccinimidyl suberate did not promote oligomerization, indicating that *Sm*YbeY acts as a monomer of ∼20 kDa (Supplementary Figure S4).

It has been reported that *Eco*YbeY acts as a metallo endoribonuclease that specifically cleaves single-stranded RNA (ssRNA) substrates (13). We therefore assayed purified *Sm*YbeY for RNase activity. The monomeric *Sm*YbeY (5 μM) was first incubated with a 5′ end-labeled 30mer ssRNA oligonucleotide in Tris-buffered solutions containing NaCl or KCl and magnesium (Mg^{2+}) as co-factor (Figure 2, left two panels). *Sm*YbeY barely cleaved this substrate in NaCl-containing buffer. However, the presence of KCl enhanced cleavage efficiency, as revealed by a marked formation of a major 3-nt degradation product. The incubation of 30mer ssRNA with a higher enzyme concentration (10 μM) resulted into an increased accumulation of several additional reaction products (Supplementary Figure S5A). We have also tested the activity of *Sm*YbeY

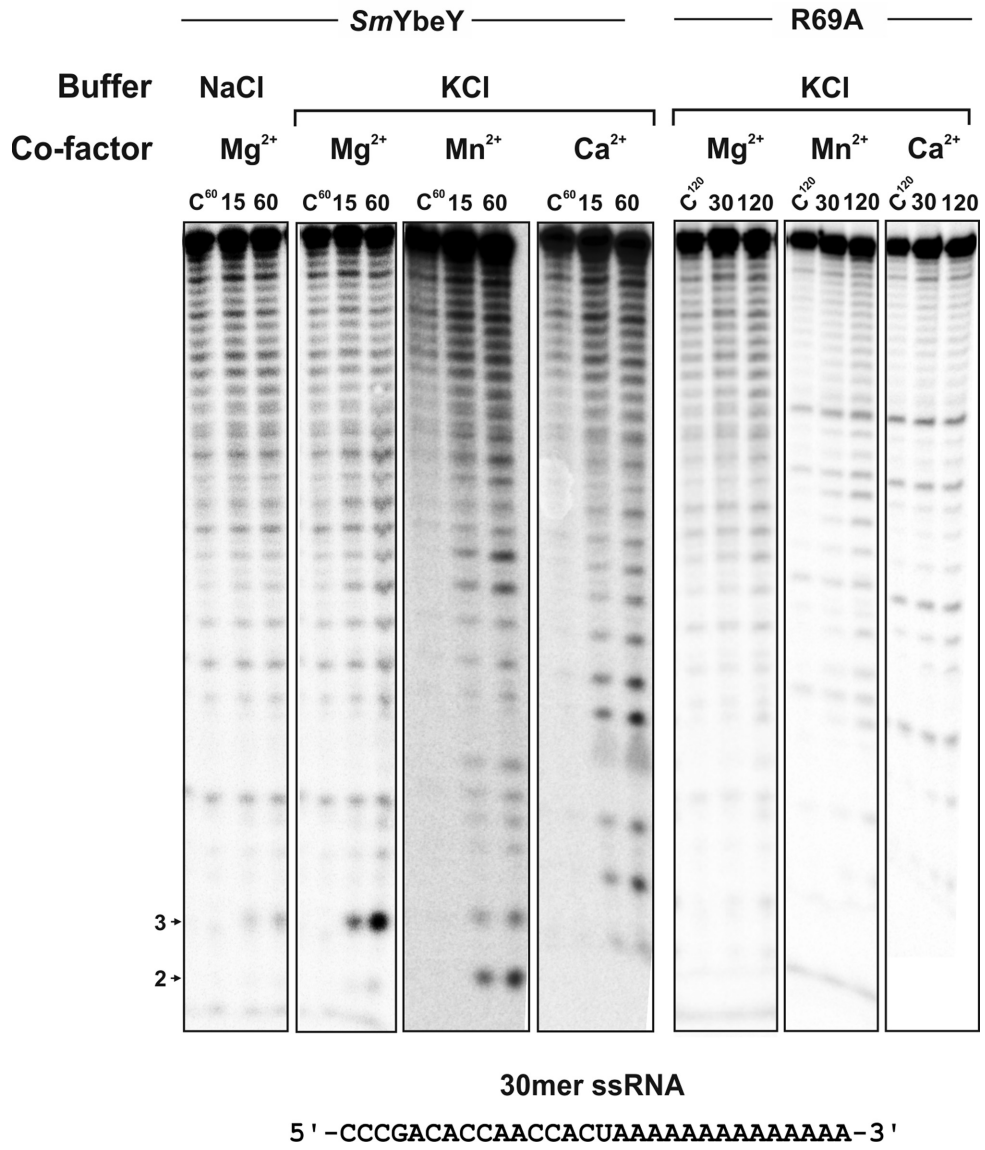

Figure 2. Activity of *Sm*YbeY on single-stranded RNA (ssRNA). *In vitro* reactivity of purified wild-type *Sm*YbeY and the mutant variant *Sm*YbeY-R69A on a 5′-labeled 30mer ssRNA oligonucleotide (0.02 pmol/μl) whose sequence is indicated on bottom. Enzymes were used at a concentration of 5 μM in all assays. Buffering conditions and incubation times are indicated on top of the panels. Numbers to the left indicate sizes of the major reaction products. Reactions were analyzed on 7 M urea/20% polyacrylamide gels. C, control reactions.

with a smaller ssRNA, the 16mer oligoribonucleotide. This RNA was also cleaved by *Sm*YbeY, although with less efficiency when compared to the 30mer (Supplementary Figure S5A), suggesting that *Sm*YbeY has preference for longer substrates. We next tested *Sm*YbeY activity on the 30mer ssRNA substrate in KCl solution with either manganese (Mn^{2+}) or calcium (Ca^{2+}) as alternative divalent metal co-factors (Figure 2). These new incubation conditions promoted 30mer ssRNA cleavage at different positions, most likely in a non-specific manner. Of note, the substitution of the ultraconserved arginine R69 (Supplementary Figure S6) by an alanine residue (*Sm*YbeY-R69A) rendered *Sm*YbeY almost inactive on this generic ssRNA substrate, which further demonstrates that the observed cleavage was protein-dependent.

It has been also shown that *Eco*YbeY does not cleave double-stranded RNA (dsRNA) (13). We tested the activity of *Sm*YbeY (5 μM) on a partially dsRNA with a single-strand 3′-poly(A) tail (30:16-ds) as well as on fully double-stranded 16mer (16:16-ds) and 39mer (39:39-ds) RNA substrates (Figure 3 and Supplementary Figure S5B). Efficient duplex formation was checked by binding shift assays in each case. *Sm*YbeY cleaved the 30:16-ds RNA unspecifically at multiple sites within its double-stranded portion, but more efficiently if Mn^{2+} was used as co-factor (Figure 3A, left two panels). In contrast, Ca^{2+} precluded *Sm*YbeY activity on this RNA substrate. The *Sm*YbeY-R69A mutant enzyme showed extremely low activity on this substrate in the presence of Mg^{2+} and Mn^{2+}, with Ca^{2+} acting also as an inhibitor, with Ca^{2+} acting also as an inhibitor

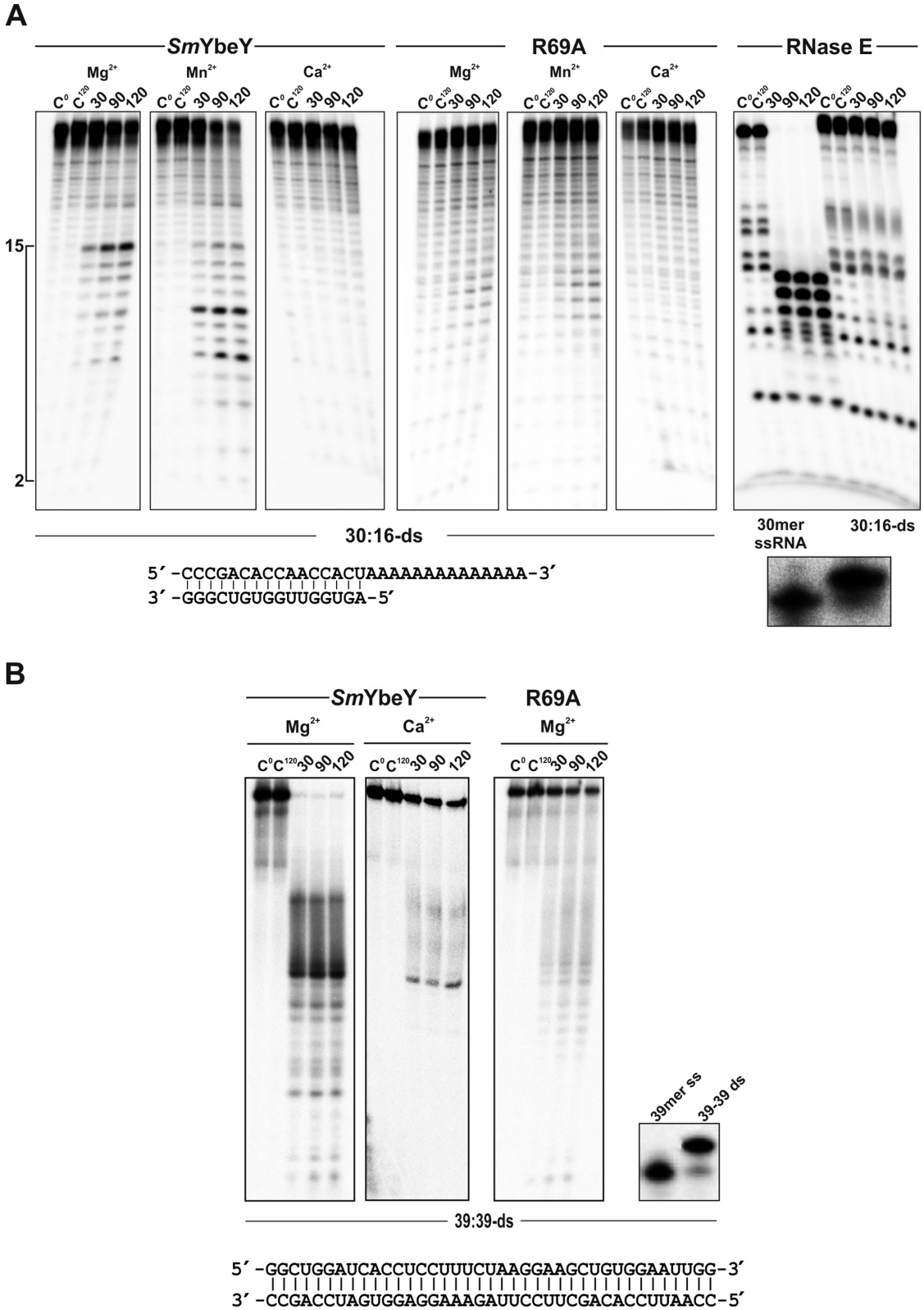

Figure 3. Activity of *Sm*YbeY on dsRNA. Enzymes were used at a concentration of 5 μM in all assays. Reactions were incubated in KCl-containing buffer in the presence of the co-factor indicated on top of the panels. Reaction times are also indicated. Cleavage products were separated on 7 M urea/20% polyacrylamide gels. C, control reactions. (**A**) *In vitro* reactivity of purified wild-type *Sm*YbeY and the mutant variant *Sm*YbeY-R69A on a partially dsRNA substrate (30:16-ds) (0.02 pmol/μl) whose sequence is indicated on bottom. The bracket to the left indicates the size range of breakdown products. RNase E was assayed with the 30:16-ds and 30mer ssRNA substrates (0.02 pmol/μl) as control of cleavage specificity on dsRNA (right panel). The gel of a shift assay (15% polyacrylamide) showing effective duplex formation is shown on bottom. (**B**) Reactivity of *Sm*YbeY and *Sm*YbeY-R69A on the 39:39-ds dsRNA substrate (0.24 pmol/μl), whose sequence is shown on bottom. Gel of the shift assay (15% polyacrylamide) showing formation of the duplex is also shown.

(Figure 3A, central panels). To further demonstrate that cleavage on the 30:16-ds RNA was *Sm*YbeY-dependent and not the result of substrate breathing we tested the activity of the single-strand specific endoribonuclease RNase E on both the 30mer ssRNA and the 30:16-ds RNA molecules at 37°C, i.e. the *Sm*YbeY reaction temperature (Figure 3A, right two panels). RNase E fully degraded the ssRNA whereas the double-stranded substrate remained unaltered at the end of the assay. The shorter 16:16-ds RNA was also cleaved by *Sm*YbeY at several positions when Mg^{2+} was used as co-factor (Supplementary Figure S5B). Remarkably, the activity of the protein was more evident on a longer dsRNA molecule (39:39-ds), which was totally consumed after 30 min of incubation of the reaction mixtures in a Mg^{2+}-containing buffer (Figure 3B). Once again, the activity of *Sm*YbeY was dramatically reduced in the presence of Ca^{2+} (Figure 3B). Similar to what was observed with the other RNA substrates, the *Sm*YbeY-R69A mutant enzyme showed residual activity on the 39:39-ds (Figure 3B).

Collectively, these results revealed that *Sm*YbeY has ribonuclease activity on both ssRNA and dsRNA substrates, although the enzyme has preference for longer dsRNA molecules. *Sm*YbeY-mediated catalysis is supported by Mg^{2+} and Mn^{2+} as divalent metal co-factors. Nonetheless, each co-factor influenced cleavage efficiency and breakdown patterns in a different manner. Ca^{2+} selectively impaired *Sm*YbeY ability to cleave dsRNA.

*Sm*YbeY cleaves structured and CoIP-enriched RNAs

We next tested the ability of *Sm*YbeY for cleaving a series of structured RNA molecules namely, the generic R1.1 RNA substrate, commonly used to assay the *in vitro* activity of the double-strand endoribonuclease RNase III (49), total rRNA and a transfer RNA (tRNA-Ser) (Figure 4). Incubation of *Sm*YbeY (5 μM) with the internally labeled 60-nt R1.1 RNA in KCl-containing buffer and Mg^{2+} as co-factor rendered two major 47-nt and 13-nt long reaction products along with a series of less abundant molecules (including 19-nt and 28-nt long products) (Figure 4A, left panels). Remarkably, the 47-nt, 28-nt, 19-nt and 13-nt long RNA species derived from cleavage at positions already reported to be preferred by RNase III within the main loop of the R1.1 substrate (50,51). There were also additional minor products that may result from cleavages on the small loop (on the top) of R1.1 (indicated with an asterisk in Figure 4A). Ca^{2+} inhibited *Sm*YbeY activity when assayed in the same concentration and buffering conditions. A higher *Sm*YbeY concentration (10 μM) and longer incubation of the reaction in the presence of Mg^{2+} resulted in a similar R1.1 breakdown pattern (Figure 4A, central panels). However, the use of Mn^{2+} as co-factor in the assays promoted almost depletion of the full-length R1.1 substrate shortly upon reaction initiation (30 min) as well as minor cleavage at additional sites within R1.1. Interestingly, although less efficiently *Sm*YbeY-R69A retained the ability of the wild-type protein for cleaving R1.1 at the major reaction sites (Figure 4A, right panel).

On the other hand, *Sm*YbeY (20 μM) was also very active in degrading total rRNA in the presence of Mg^{2+}, Mn^{2+} and Ca^{2+} (Figure 4B, left panel). We have shown that Ca^{2+} inhibited cleavage of *Sm*YbeY on the structured R1.1. RNA but not on ssRNA, therefore, this result suggests that the enzyme likely recognizes the larger stems within the complex structured rRNAs as single-stranded substrates. The R69A mutation strongly attenuated reactivity of *Sm*YbeY on rRNA whereas EDTA (50 mM) totally blocked RNase activity, further supporting that *Sm*YbeY is a metal-dependent endoribonuclease. Given that *Eco*YbeY has been shown to be involved in 16S rRNA maturation (13) we also assayed the activity of *Sm*YbeY on an *in vitro* synthetized 39-nt RNA substrate that mimics the sequence of the 3′ terminus of the *S. meliloti* 16S rRNA precursor (Supplementary Figure S7). *Sm*YbeY reacted poorly with this RNA molecule in the conditions tested (Mg^{2+} as co-factor) (Supplementary Figure S7A). Consistent with this finding, the Sm*Δybe Y* mutant showed an unaltered wild-type rRNA profile even upon a temperature upshift (Supplementary Figure S7B). Similarly, only minor products were detected after incubation of *Sm*YbeY with the structured 89-nt long tRNA-Ser substrate (Figure 4B, right panels).

These findings confirmed the previous observations that *Sm*YbeY is able to cleave a diversity of structured RNA molecules. Moreover, and contrary to what was observed in *E. coli*, *Sm*YbeY does not seem to be involved in 16S rRNA maturation.

Finally, in a new series of *in vitro* experiments we also incubated *Sm*YbeY with endogenous *S. meliloti* substrates, i.e. the *ybe Y* and *ugpA* mRNAs, and the SMa_asRNA_345 asRNA (Figure 5). The two latter transcripts were selected because of their enrichment in CoIP-RNA, i.e. 3.20- and 2.07-fold with respect to the control, respectively. *Sm*YbeY was extremely effective in cleaving all these three RNA molecules, with total consumption of the substrates early (30 min) after the start of the reactions. These results validate the CoIP–RNA described above as a resource to identify *Sm*YbeY substrates.

*Sm*YbeY influences chromosome-linked and symbiotic plasmid pathways

We also investigated the *Sm*YbeY-dependent molecular responses of *S. meliloti* by profiling the transcriptomes of the Sm2B3001 strain and its deletion mutant derivative Sm*Δybe Y* on Sm14kOLI microarrays (Supplementary Tables S4 and S5). To unequivocally demonstrate that the observed changes in the transcriptome were exclusively due to the lack of *Sm*YbeY we sequenced the genomes of the parent and mutant strains, which confirmed the in-frame deletion of *ybe Y* and the absence of second site suppressor mutations in Sm*Δybe Y* (Supplementary Figure S1). Accordingly, the growth phenotypes of the Sm*Δybe Y* mutant in complete TY and minimal MM media were complemented with plasmid pJBYbeY, which expresses *ybe Y* from its own promoter (Supplementary Figure S2). Total RNA was then obtained from bacteria grown to exponential (log RNA) and stationary (stat RNA) phase in complete TY medium. These experiments identified 543 and 209 *Sm*YbeY-dependent mRNAs (i.e $-1 \geq M \geq 1$) in log and stat RNA samples, respectively, with 86 of those common to both growth states. Therefore, in our experimental condi-

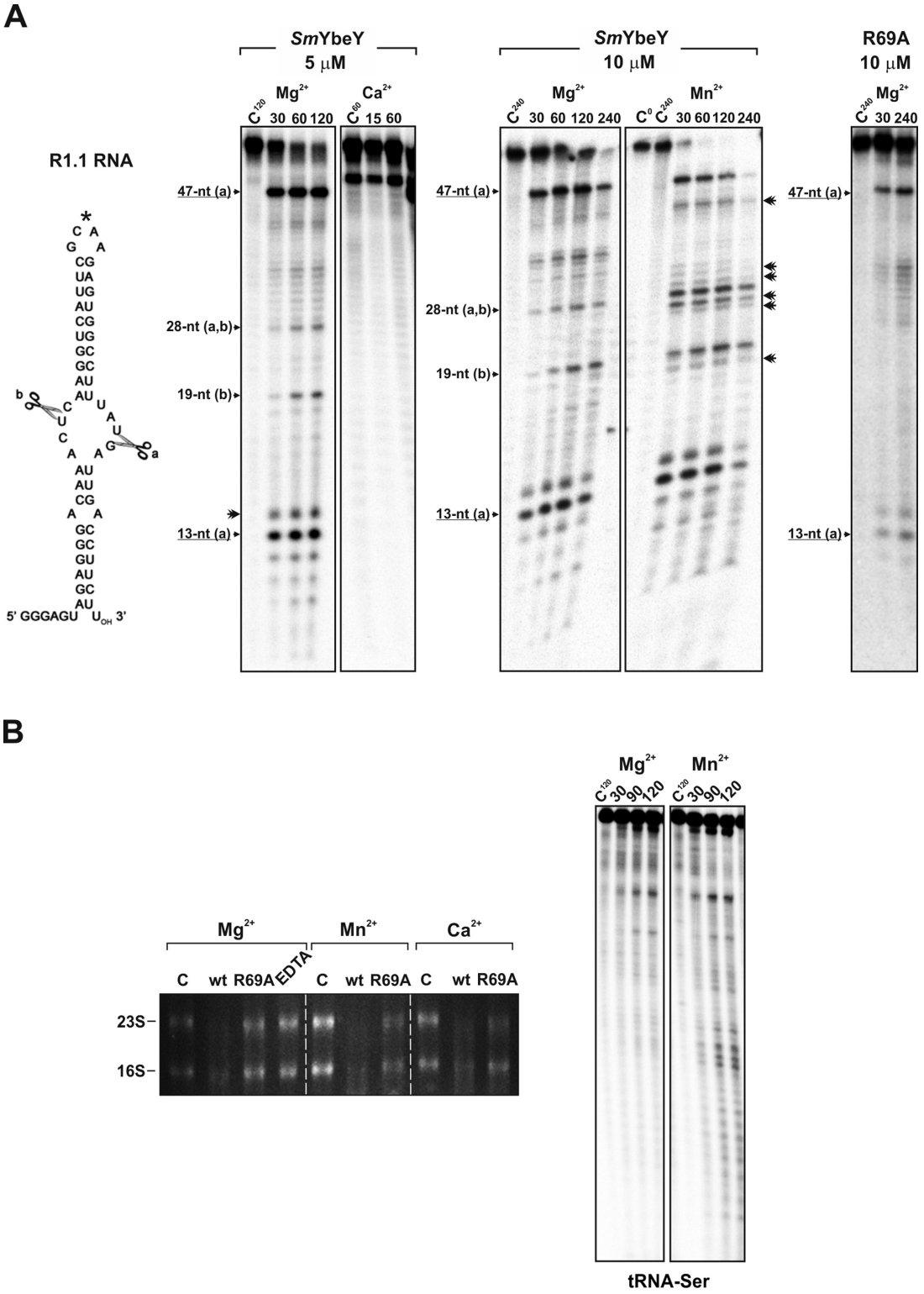

Figure 4. Activity of *Sm*YbeY on structured RNA substrates. (**A**) Reactivity patterns of *Sm*YbeY and *Sm*YbeY-R69A on the R1.1 RNA (1.12 pmol/μl), the canonical substrate for RNase III. Sequence and secondary structure of the substrate is shown to the left. Enzyme concentrations, metal co-factor and reaction times are indicated on top of the panels. Reactions were analyzed on 7 M urea/15% polyacrylamide gels. Known cleavage sites (A and B) of RNase III on the same substrate are indicated. The asterisk (*) indicates an alternative minor cleavage site within R1.1. Additional minor reactions products when Mn^{2+} was used as co-factor are indicated by double arrowheads. C, control reactions. (**B**) Left panel, activity of *Sm*YbeY and *Sm*YbeY-R69A on rRNA (500 ng). Enzymes (20 μM) were incubated for 2 h at 37°C in the presence of EDTA (50 mM) and/or the co-factors indicated on top. RNA was analyzed on a 1.5% agarose gel. The positions of the 23S and 16S rRNA are indicated. C, control reactions. Right panels, activity of *Sm*YbeY (10 μM) on tRNA-Ser. Metal co-factors used in the assays and the time-course of the reactions are indicated on top of the panels. The reaction products were separated on 7 M urea/10% polyacrylamide gels. C, control reactions.

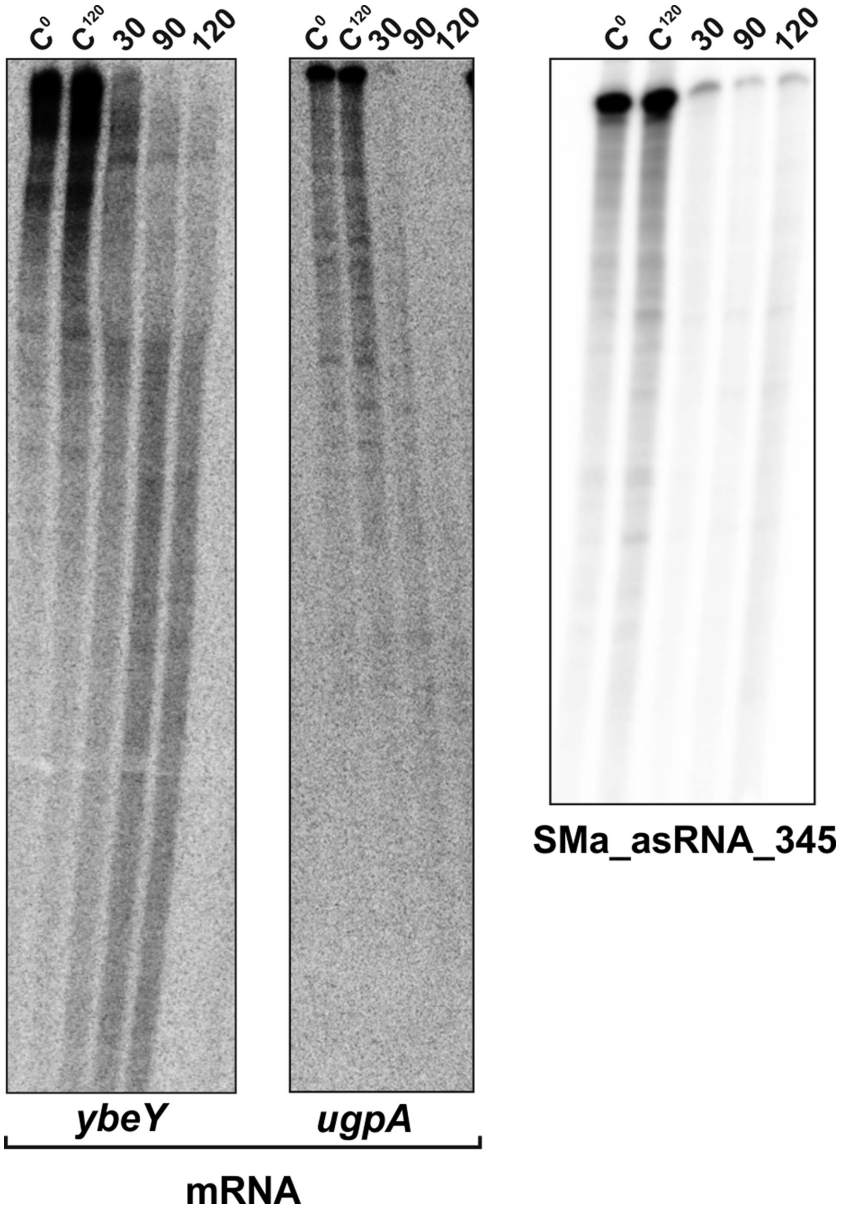

Figure 5. Activity of *Sm*YbeY on endogenous *S. meliloti* substrates. *Sm*YbeY efficiently cleaves *ybeY* (0.03 pmol/μl) and *ugpA* (0.2 pmol/μl) mRNAs (left panel) and the asRNA SMa_asRNA_345 (0.02 pmol/μl) (right panel). Reactions were analyzed on 7 M urea/8% polyacrylamide (mRNAs) or 7 M urea/10% polyacrylamide (asRNA) gels. Concentration of the enzyme in the assays was 10 μM and the reaction mixtures were incubated in the presence of Mg^{2+}. Incubation times are indicated on top of the panels. C, control reactions.

tions lack of *Sm*YbeY altered the expression of 666 protein-coding genes (∼11% of the *S. meliloti* Rm1021 ORFs) (Supplementary Table S4). Functional clustering of these genes revealed that 39.8% encode metabolic functions, 11.1% are related to translation and RNA turnover and 16.5% represent widely diverse cellular processes (e.g. motility, signal transduction and transcription, transposition or nitrogen-fixation) (Figure 6A and Supplementary Figure S8). The remaining 32.6% have unpredictable function. Differential accumulation of a subset of representative mRNAs displaying M values ranging from −2.5 to 2.0 was further confirmed by qRT-PCR analysis (Supplementary Table S6).

Sm14kOLI microarrays can also probe most of the recently identified *S. meliloti* non-coding RNAs (ncRNAs). Specifically, we have estimated that at least 478 known *trans*-sRNAs have oligonucleotide probes in these microarrays. Analysis of the hybridization signals on this set of probes revealed that lack of *Sm*YbeY altered the expression of 131 and 77 ncRNAs during exponential and stationary bacterial growth, respectively, with 17 of those present in both data sets (Supplementary Table S5). The majority (72.3%) of these ncRNAs corresponded to putative *cis*-acting sense transcripts (i.e. 5′/3′-UTRs of mRNAs), whereas *trans*-sRNAs represented 19.4%, asRNAs 5.2% and tRNAs 3.1% (Figure 6A and Supplementary Figure S8). Therefore, *Sm*YbeY does not seem to have a major role at least in *trans*-sRNA turnover. Our experimental approach underestimates the expression of asRNAs since only

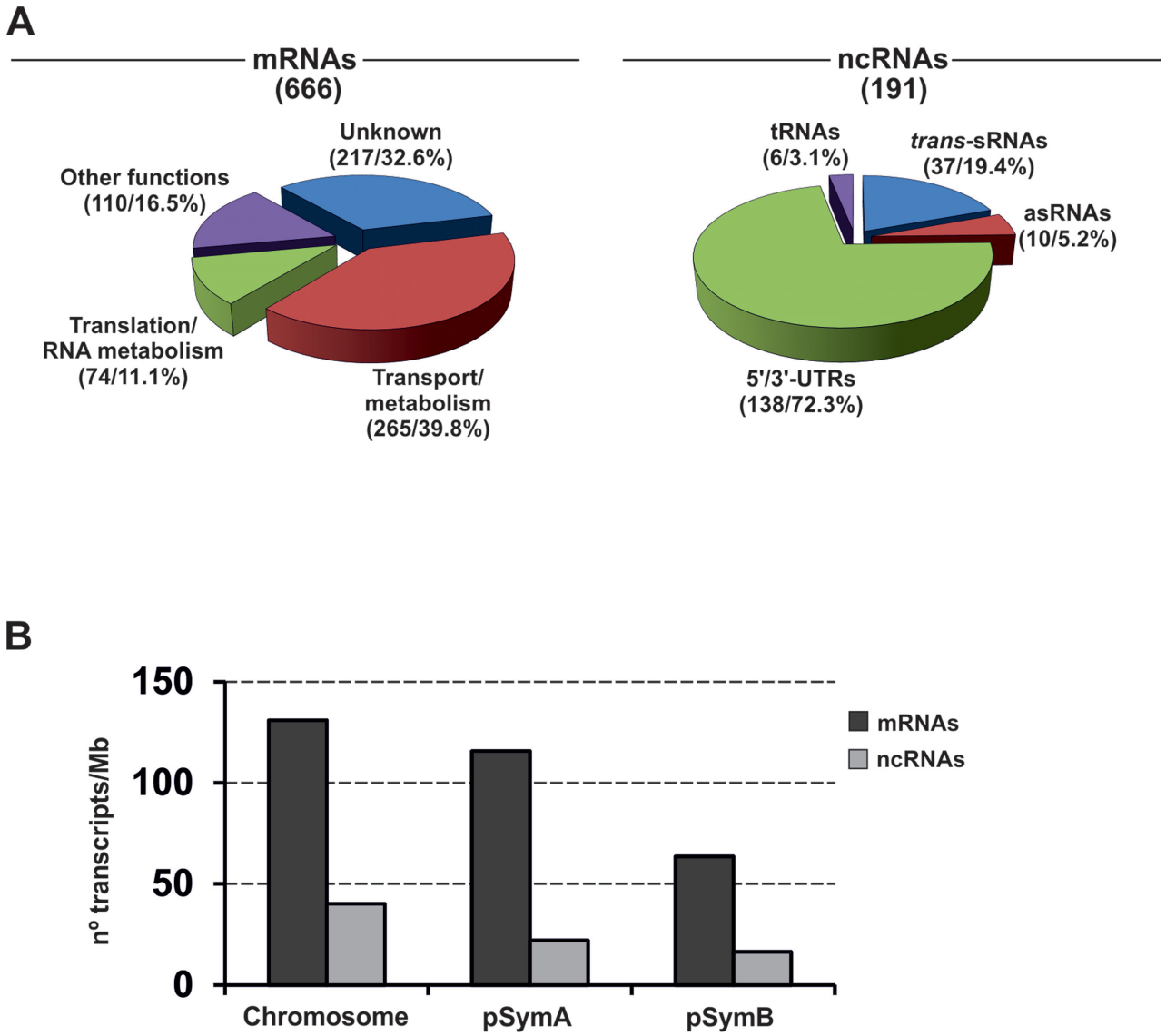

Figure 6. *Sm*YbeY-dependent alteration of the *S. meliloti* transcriptome. (**A**) Number and functional categories of mRNAs and non-coding RNAs (ncRNAs) differentially accumulated in the Sm*Δybe Y* mutant. (**B**) Impact of *Sm*YbeY on the accumulation of chromosomal, pSymA and pSymB mRNAs and ncRNAs. The histogram shows the number of differentially expressed transcripts per Mb in each replicon.

a subset of these transcripts (i.e. those antisense to 5′/3′-UTRs of mRNAs) are represented in the Sm14kOLI microarrays, which precludes a conclusion about the influence of *Sm*YbeY in asRNA accumulation.

The *S. meliloti* genome consists of three large replicons, the chromosome (3.7 Mb) and the symbiotic megaplasmids pSymA (1.4 Mb) and pSymB (1.7 Mb). Interestingly, distribution of the differentially accumulated mRNAs in this genome revealed a similar relative impact of *Sm*YbeY activity on the expression of chromosomal and pSymA-borne genes (Figure 6B). Chromosomal *Sm*YbeY-dependent genes included those related to ribosome biogenesis, translation, RNA turnover, energy metabolism and flagellum assembly (Figure 7A). Specifically, *Sm*YbeY loss-of-function resulted in pervasive down-regulation during both exponential and stationary growth of a set of genes coding for most of the ribosomal proteins, a set of elongation/translation initiation factors and tRNA synthetases as well as the ribonucleases RNase P, PNPase, RNase III and RNase D. A similar expression profile was exhibited by a number of genes involved in ATP synthesis and cytochrome C oxidase assembly. However, transcripts encoding substrate-dependent dehydrogenases and oxidoreductases showed variable accumulation in the Sm*Δybe Y* mutant. Microarray data also revealed up-regulation in this mutant of gene clusters coding for flagellar structural elements, particularly upon entry of bacteria into stationary phase. This misregulation of flagella biosynthesis most likely explains the reduced swimming motility of the Sm*Δybe Y* mutant with respect to the parent strain (Supplementary Table S7).

S. meliloti symbiotic plasmid pSymA mostly encodes functions contributing to ecological specializations of this bacterium, e.g. microaerobic nitrate respiration and sym-

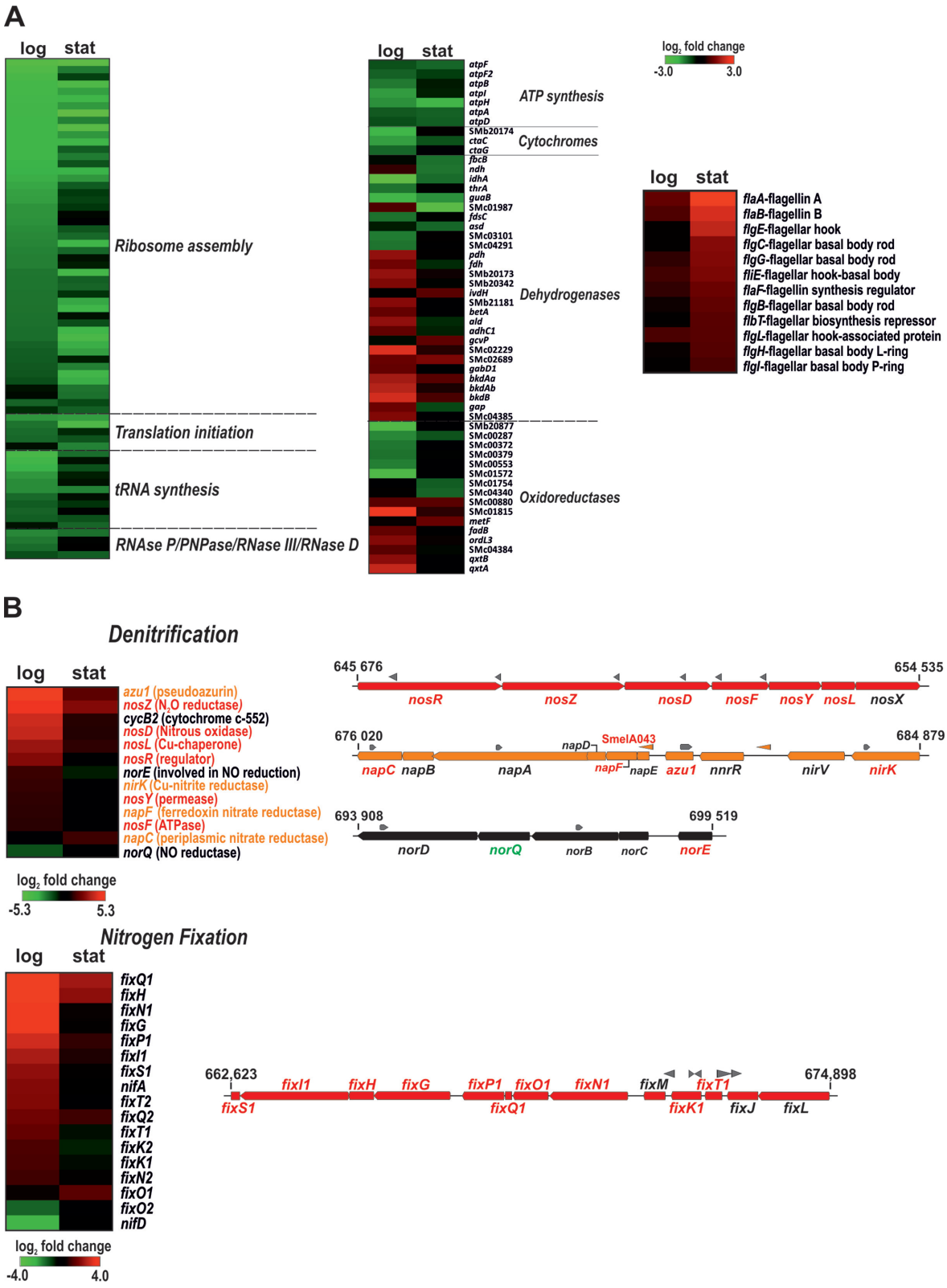

Figure 7. Core and plasmid pathways influenced by *Sm*YbeY. Changes in mRNA abundance in exponential (log) and stationary (stat) cultures are visualized in heatmaps generated with the MeV tool (http://www.tm4.org/mev.html). In the color scale (log_2 fold changes) green and red stand for down- and up-regulation in the SmΔ*ybeY* mutant, respectively. (**A**) Chromosomal genes related to translation and RNA turnover (left), energy metabolism (middle) and flagella biosynthesis (right). (**B**) Genes of symbiotic plasmid pSymA involved in anaerobic denitrification (upper panel) and nitrogen-fixation (bottom panel). Gene clusters specifying each pathway are depicted to the side of each panel. Grew arrowheads stand for annotated asRNAs. The names of differentially expressed genes within each operon are colored.

biotic nitrogen fixation (Figure 7B). A number of genes coding for proteins involved in the denitrification pathway including the nitrate, nitrite and nitrous oxide reductases NapC, NirK and NosZ, respectively, were strongly up-regulated in exponentially growing SmΔ*ybeY* mutant bacteria. Similar influence of *Sm*YbeY was observed on the expression of genes coding for the master regulators of nitrogen fixation (i.e. FixK1/2 and NifA) and the elements of the electron transport chain associated with the nitrogenase activity, i.e. most of the genes integrating the *fixNOQPGHIS* operon. The accumulation profiles of these two sets of transcripts indicate an involvement of *Sm*YbeY in the post-transcriptional silencing of denitrification and nitrogen fixation under free-living non-symbiotic conditions.

Discrete overlap between the Hfq- and *Sm*YbeY-dependent genes

Published data have evidenced large similarities between the physiological phenotypes associated to *Sm*YbeY and Hfq loss-of-function in *S. meliloti*, which has been interpreted as the consequence of a strong functional relation between the two proteins (3,10,28). To further explore these commonalities at the molecular level we have compared the Hfq- and *Sm*YbeY-dependent gene sets (Figure 8). The latter included the 255 *Sm*YbeY-bound mRNAs identified in the CoIP experiments (Supplementary Table S3), of which 23 (9%) were also scored as differentially expressed in the SmΔ*ybeY* mutant. Accumulation of almost half of these 23 transcripts, including the *ugpA* mRNA (Figure 5), was negatively influenced by *Sm*YbeY and therefore could be preferred substrates for this endoribonuclease (Supplementary Table S4). Nonetheless, the reduced overlap between these two data sets could be mostly explained by the differences in the experimental setups, i.e. transcriptomics were only performed in two out of the five culture conditions used in the CoIP experiments.

The compilation of existing transcriptomics and proteomics data uncovered a large Hfq regulon integrated by 917 protein-coding genes (35,52–54) of which 197 (~21%) were also scored in this study as differentially expressed in the SmΔ*ybeY* mutant. Interestingly, 93 of these genes code for mRNAs that have recently been reported to bind Hfq (26). Conversely, most of the 202 *Sm*YbeY mRNA ligands have been previously catalogued as Hfq-independent. Within the subset of 93 Hfq/*Sm*YbeY co-regulated genes, 69 encode proteins with predictable function, namely 26 involved in metabolism, 8 in translation, 10 in nutrient uptake, 6 in flagella biosynthesis, 5 in symbiotic nitrogen-fixation, 4 in denitrification and 9 in transcription and/or signal transduction (Figure 8). These 69 genes can be grouped into two major categories according to their expression patterns in the Hfq and *Sm*YbeY mutants; (i) genes that exhibited opposite dependence on Hfq and *Sm*YbeY activity, being mostly up-regulated in SmΔ*ybeY* and consistently down-regulated in the different Hfq mutant strains (41 genes), and (ii) genes whose expression is negatively influenced by both proteins (17 genes) and therefore have been catalogued as up-regulated in the respective mutants. The first category includes large fractions of metabolic and regulatory genes and the full subsets of genes coding for proteins involved in denitrification, nitrogen fixation, biosynthesis of flagella and sugar transport. These mRNAs may be protected by Hfq from *Sm*YbeY-mediated degradation. The second major group of Hfq/*Sm*YbeY-dependent genes codes for either metabolic proteins or amino acid transporters. *Sm*YbeY would be involved in the decay of these mRNAs upon translational inhibition by Hfq-dependent *trans*-acting sRNA partners.

Overall, this comparative analysis revealed a discrete overlap between Hfq- and *Sm*YbeY-dependent genes. Nonetheless, it enabled the prediction of putative Hfq-dependent and independent *Sm*YbeY substrates among the mRNAs exhibiting increased steady-state levels in the SmΔ*ybeY* mutant.

*Sm*YbeY is required for the sRNA-mediated silencing of amino acid ABC transporters

Accumulation of some known Hfq-binding mRNAs encoding periplasmic components of amino acid ABC transporters is negatively influenced by both Hfq and *Sm*YbeY. The Hfq-dependent *trans*-sRNAs AbcR1 and AbcR2 have among their experimentally confirmed targets two of these mRNAs, namely *prbA* and *livK*, which code for proline betaine and branched-chain amino acid transporters, respectively (26,37). In particular, our transcriptomics profiling revealed that levels of the *prbA* mRNA increased more than 5-fold in the SmΔ*ybeY* mutant with respect to the wild-type strain during exponential growth, suggesting that the post-transcriptional silencing of *prbA* requires *Sm*YbeY. However, the *prbA* mRNA was not recovered in the CoIP–RNA. Therefore, we further investigated the putative role of *Sm*YbeY in the regulation of *prbA* mRNA and if this layer of regulation is AbcR2-dependent.

Northern hybridization of total RNA from rifampicin-treated cells confirmed that lack of *Sm*YbeY has no effect on either processing or stability of AbcR2 (Supplementary Figure S9). Thus, we hypothesized that *Sm*YbeY may influence *prbA* decay upon its predicted antisense interaction with AbcR2. To test this hypothesis we measured the *Sm*YbeY- and AbcR2-dependent fluorescence of exponential cultures of a series of reporter strains expressing constitutively from pR*prbA*::eGFP (26) a translational fusion of 211-nt of the *prbA* mRNA 5′ region, which contains the predicted AbcR2 interaction site, to eGFP (Figure 9A). First, the Sm2B3001 strain and its SmΔ*ybeY* derivative were transformed with the control plasmid pBBsyn–eGFP, expressing constitutively eGFP with a *prbA*-unrelated 5′-UTR or pR*prbA*::eGFP. Fluorescence of the control construct was ~25% (statistically non-significant) lower in the mutant than in the wild-type background, probably due to eGFP mistranslation. In contrast, fluorescence of pR*prbA*::eGFP increased more than 50% in the SmΔ*ybeY* strain. These results confirmed the *Sm*YbeY-dependent post-transcriptional regulation of *prbA* and rendered the 5′ region of the mRNA as the specific target of this regulation. We next mobilized pR*prbA*::eGFP to the AbcR1/2 deletion mutant Sm2B2001ΔR1/2 and to the SmΔR1/2Δ*ybeY* triple mutant (i.e. devoid of the AbcR1/2 and *ybeY loci*), both harboring the compatible control empty plasmid pSRK-C or pSRK-R2, the latter expressing AbcR2 consti-

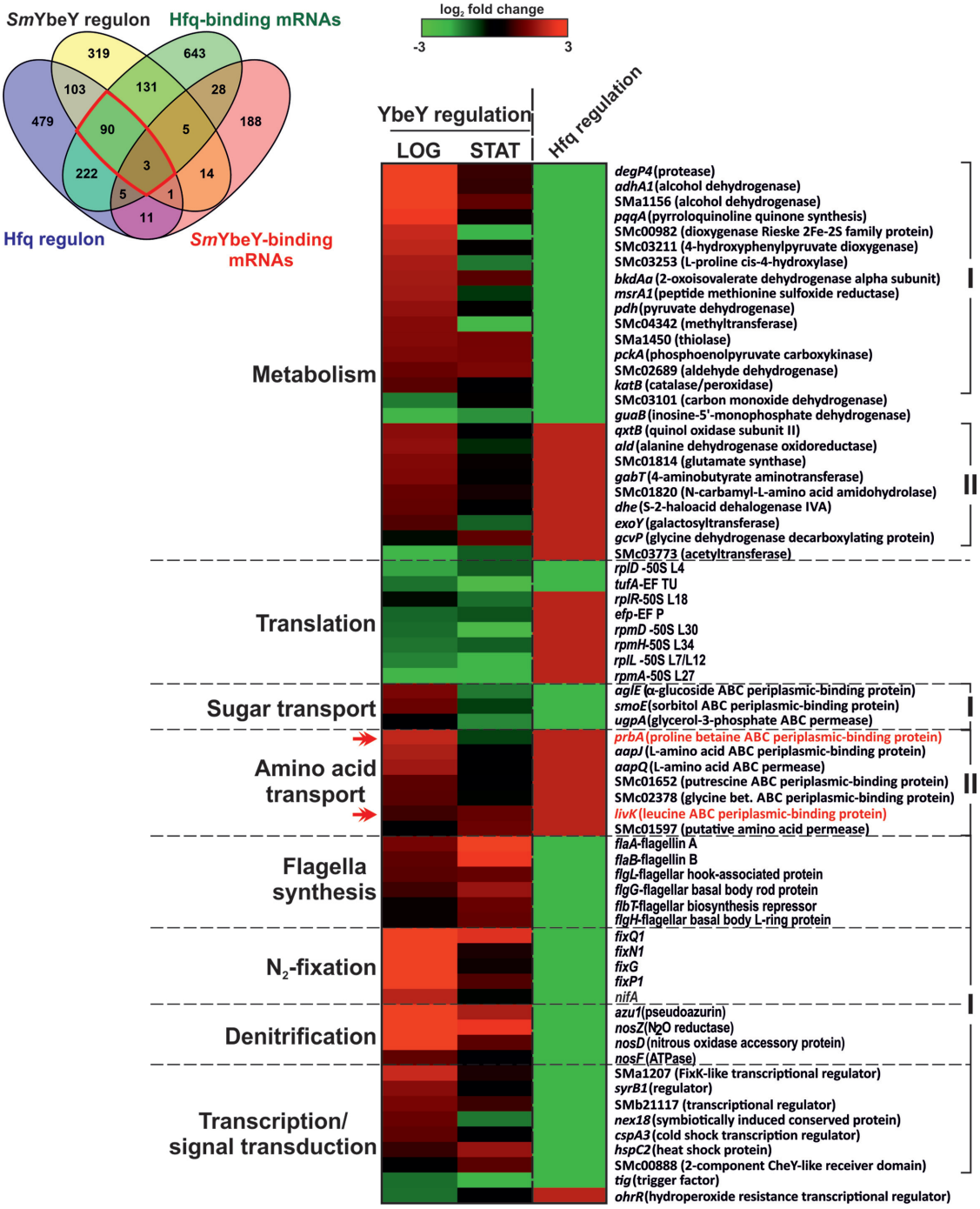

Figure 8. Overlap between the Hfq- and *Sm*YbeY-dependent gene sets in *S. meliloti*. On the left, Venn-diagram representing Hfq- and *Sm*YbeY-binding mRNAs and the transcripts differentially accumulated in the respective mutant strains. Hfq data sets were compiled from the literature. The red box indicates the 93 Hfq-*Sm*YbeY co-regulated mRNAs that are known to bind the Hfq chaperone. On the right, heatmap illustrating accumulation in the *Sm*YbeY and Hfq mutants of a subset of these 93 mRNAs (69) that encode proteins with predictable function. Functional categories are indicated to the left and the identity of each gene to the right of the panel. In the color scale (log_2 fold changes) green and red stand for down- and up-regulation in the mutants, respectively. Due to the heterogeneity of Hfq data sets fixed values of −3 and 3 were applied for the Hfq-dependent genes. I, genes inversely regulated by Hfq and *Sm*YbeY; II, genes negatively influenced by both proteins. Double arrowheads in red indicate *prbA* and *livK* mRNAs, which are experimentally confirmed targets of the homologous *trans*-sRNAs AbcR1 and AbcR2.

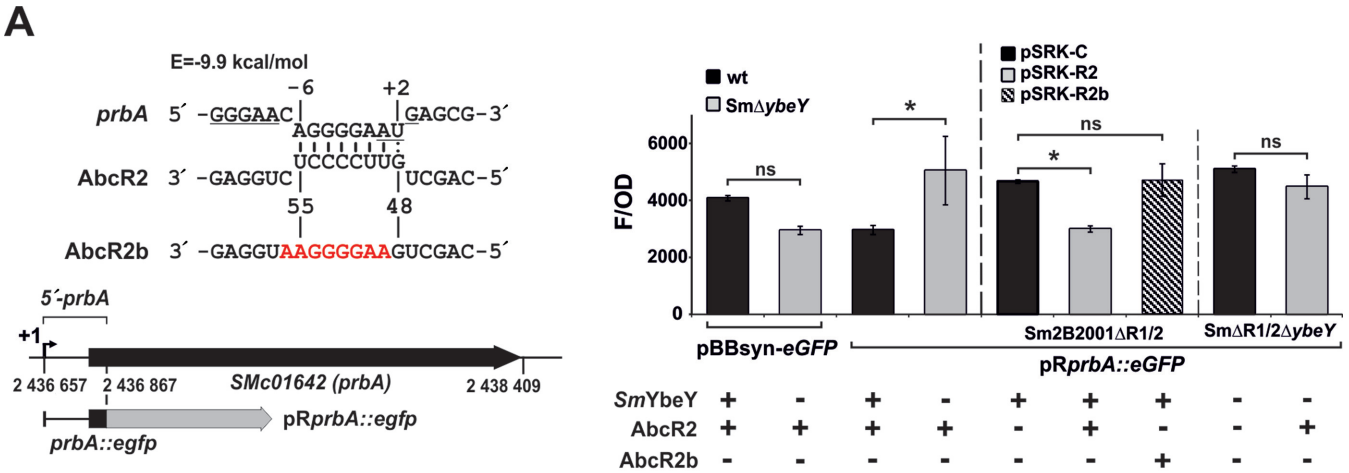

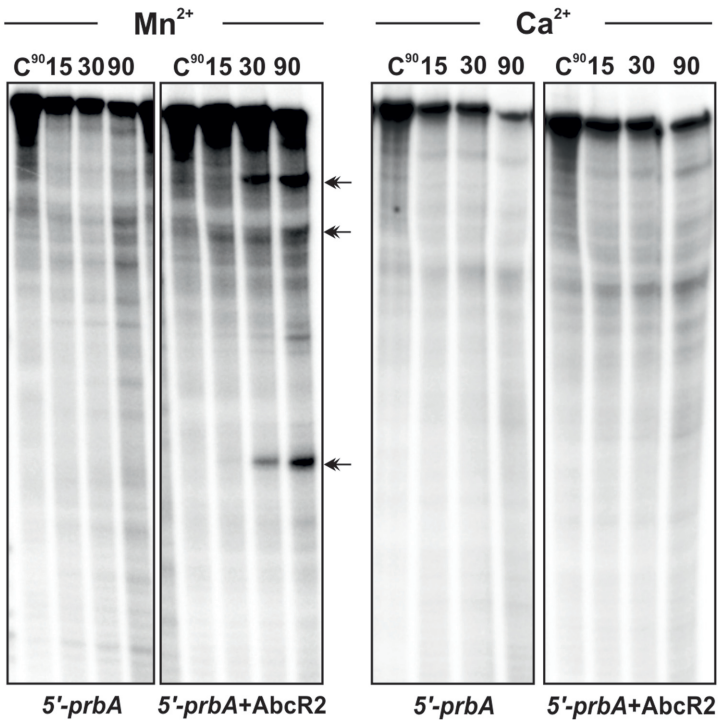

Figure 9. *Sm*YbeY is required for the AbcR2-mediated silencing of the *prbA* mRNA. (**A**) Lack of *Sm*YbeY abrogates AbcR2-dependent post-transcriptional repression of *prbA in vivo*. The AbcR2-*prbA* antisense interaction as predicted by IntaRNA (http://rna.informatik.uni-freiburg.de/IntaRNA/Input.jsp) is shown on top. The Shine–Dalgarno sequence and AUG start codon of *prbA* are underlined. Numbers indicate positions relative to the *prbA* start codon and AbcR2 transcription start site. The predicted minimum hybridization energy (E) of the duplex is indicated. Nucleotide substitutions in the AbcR2b mutant variant disrupting base-pairing with *prbA* are colored in red. The schematics below show the *prbA* genomic region and the reporter fusion used in the *in vivo* assays. Numbers stand for coordinates in the genome of the reference strain Rm1021. The transcription start site of *prbA* is indicated (+1). Histogram; fluorescence of the Sm2B3001 strain and its SmΔ*ybeY* mutant derivative transformed with the control plasmid pBBsyn-eGFP or the reporter pR*prbA::eGFP* (left part) and fluorescence of the double Sm2B2001ΔR1/2 and triple SmΔR1/2Δ*ybeY* mutants co-transformed with pR*prbA::eGFP* and pSRK-C (control), pSRK-R2 or pSRK-R2b. Values reported are means and standard deviation of 27 fluorescence measurements normalized to the OD of the culture, i.e. three determinations of three independent exponential cultures of three transconjugants for each reporter strain. The statistical significance level was set at $P < 0.05$ and indicated with an asterisk. ns, non-significant. *Sm*YbeY, AbcR2 and AbcR2b genotypes of the reporter strains are indicated on the bottom of the histogram. (**B**) *Sm*YbeY cleaves the AbcR2-*prbA* duplex *in vitro*. Reactivity patterns of *Sm*YbeY (5 μM) on an internally labeled 5′-*prbA* RNA (0.1 pmol/μl) either alone or in the presence of a molar excess of AbcR2. Double arrow heads indicate major cleavage products. Reactions were incubated in the presence of Mn^{2+} or Ca^{2+} as co-factor. Incubation times are indicated on top of the panels. Reactions were analyzed on 7 M urea/15% polyacrylamide gels. C, control reactions.

tutively (Figure 9A, right histogram). Fluorescence of exponentially growing Sm2B2001ΔR1/2 bacteria co-expressing AbcR2 and *prbA*::eGFP decreased by 35% (statistically significant) with respect to that of the same strain co-transformed with the target fusion and the empty vector pSRK-C. Further, an AbcR2 mutant variant (AbcR2b) carrying nucleotide substitutions in the predicted *prbA* interaction site and stably expressed from pSRK-R2b (Supplementary Figure S10) had no effect on the fluorescence of the reporter fusion. These results confirmed the AbcR2-mediated post-transcriptional down-regulation of *prbA*, already reported in the closely related *S. meliloti* strain Rm1021 (26). In contrast, lack of *Sm*YbeY almost abrogated repression of *prbA* by AbcR2, i.e in the triple mutant background fluorescence of pR*prbA*: eGFP hardly decreased to 12% (statistically non-significant) with respect to that of the control upon AbcR2 expression.

Finally, we tested the *in vitro* activity of *Sm*YbeY (5 μM) on an internally labeled RNA substrate that mimics the 5′ *prbA* region (5′-*prbA*) fused to eGFP both alone and upon its incubation with a molar excess of the AbcR2 transcript in the presence of Mn^{2+} as co-factor (Figure 9B). In these conditions, *Sm*YbeY hardly reacted with the 5′-*prbA* molecule, further suggesting that the *prbA* mRNA is not a preferred ligand of this protein. In contrast, addition of AbcR2 to the reaction mixture favored cleavage of the complex at precise sites within 5′-*prbA*, yielding three major cleavage products. As expected, Ca^{2+} blocked *Sm*YbeY activity on the partially double-stranded *prbA*-AbcR2 molecule.

We therefore conclude that post-transcriptional regulation of *prbA* mRNA requires *Sm*YbeY, which could be most likely involved in the decay of the message upon its antisense interaction with the Hfq-dependent *trans*-acting AbcR2 sRNA.

DISCUSSION

Here, we have shown that the *S. meliloti* YbeY protein is a divalent ion-dependent single- and double-strand endoribonuclease whose activity influences core RNA metabolism, energy producing pathways and plasmid-encoded symbiotic functions. Profiling of the *Sm*YbeY-dependent genes and RNA ligands envisaged a number of putative substrates for this RNase. Although our data revealed that Hfq and *Sm*YbeY participate in largely independent RNA networks, we provide evidences that the Hfq-dependent sRNA-mediated silencing of amino acid transport requires *Sm*YbeY. Figure 10 summarizes the insights into the cellular pathways influenced by *Sm*YbeY as revealed by our study.

*Sm*YbeY acts as versatile single- and double-strand endoribonuclease

Hfq is now viewed as a major RNA chaperone in bacteria that binds to and promotes stability of large sets of mRNA and sRNA transcripts (21). Given the apparent functional overlap between Hfq and *Sm*YbeY in *S. meliloti* and the homology of *Sm*YbeY to the MID RNA-binding domain of AGO proteins (10), we profiled the subpopulation of transcripts co-immunoprecipitated with a tagged version of *Sm*YbeY. This approach has been proved successful for the generation of accurate and reliable genome-wide atlas of Hfq RNA ligands and sRNA–mRNA regulatory pairs in *S. meliloti* and other phylogenetically distant bacterial species (26,55–60). *Sm*YbeY CoIP–RNA was barely enriched in RNA species in comparison to the number of transcripts stably bound by Hfq in the same conditions. This enrichment profile supports a major function of *Sm*YbeY as a catalytic enzyme rather than an Hfq-like role as stabilizer and facilitator of RNA–RNA interactions *in vivo*. Therefore, other methods with enhanced sensitivity are required for the accurate genome-wide mapping of *Sm*YbeY contacts of catalytic nature on RNA substrates.

To date, only the *E. coli* and *V. cholerae* YbeY orthologs have been demonstrated to have RNase activity *in vitro* (8,13), both exhibiting similar catalytic features. Although performed under experimental conditions different to those described for the former enzymes (e.g. reaction buffer or enzyme/substrate ratio), our assays similarly revealed catalytic activity of *Sm*YbeY on generic and endogenous RNA molecules, but uncovered remarkable differences in its substrate specificity with respect to the well-characterized *Eco*YbeY. The latter behaves as a single-strand specific endoribonuclease unable to degrade dsRNA but exhibiting activity on short RNA hairpins and complex structured RNA (e.g. rRNA) (8,13). *Sm*YbeY was proficient in cleaving ssRNA, dsRNA and a number of structured RNA substrates. To the best of our knowledge this versatility is an unprecedented feature among bacterial endoribonucleases (61). Nonetheless, the *in vitro* characterization of *Sm*YbeY activity suggests a preference of the enzyme for longer double-stranded and structured RNA substrates. Its cleavage pattern on ssRNA and short dsRNA is reminiscent of non-specific endoribonucleases, such as RNase E. However, despite of being non-specific, RNAse E has a bias for cleaving AU-rich regions (62). In contrast, our experimental data did not reveal any preferred cleavage site of *Sm*YbeY in these substrates. Of note, the substitution of the ultra-conserved R69 residue (R59 in *Eco*YbeY), which inhibits *Eco*YbeY activity, similarly impaired *Sm*YbeY cleavage on most substrates. However, this mutated version retained reliable residual activity in some structured RNA molecules tested (e.g. R1.1). Together with the finding that *Sm*YbeY is also a double-strand endoribonuclease, this suggests that the catalytic mechanisms of both *E. coli* YbeY and the *S. meliloti* homologue may differ.

Under optimal assay conditions *Sm*YbeY completely degraded the hairpin-structured R1.1 RNA substrate at sites recognized by the prototypical double-strand endoribonuclease RNase III (50,51). The catalytically competent form of RNase III is a homodimer in which each subunit coordinates a divalent metal ion (preferably Mg^{2+}) and contributes to the hydrolytic cleavage of one strand of the duplex RNA substrate (63). YbeY and RNase III polypeptides are structurally unrelated (9,10,52). Indeed, our results indicated that *Sm*YbeY does not dimerize and thus, a ∼20 kDa monomer is likely the active form of the enzyme. Co-factor requirements of *Eco*YbeY have not been stablished yet. However, we have shown that the *in vitro* reactivity patterns and performance of *Sm*YbeY largely depend on

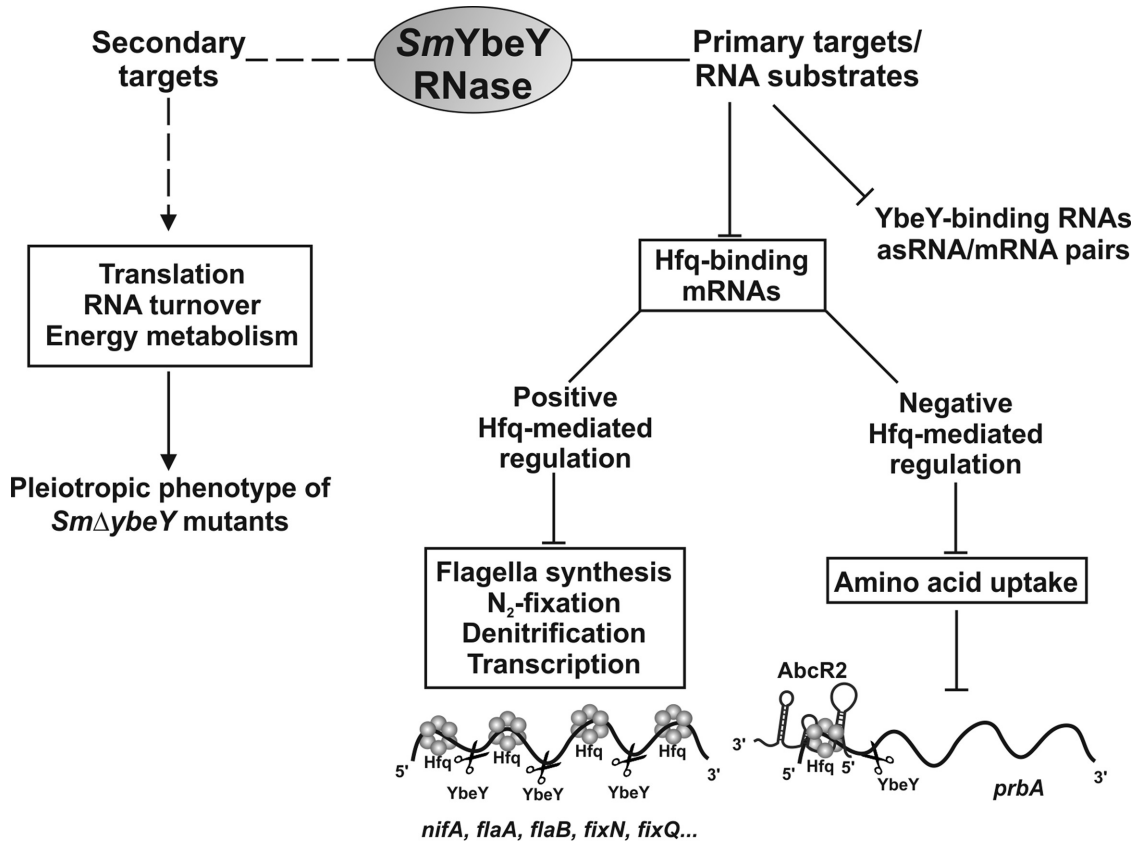

Figure 10. The *Sm*YbeY mRNA network. The scheme summarizes the impact of *Sm*YbeY on the *S. meliloti* transcriptome and its functional consequences. See discussion for details.

the divalent metal ion used in the assays. Both Mg^{2+} and Mn^{2+} supported *Sm*YbeY-mediated catalysis, but Mn^{2+} increased the overall cleavage efficiency. On the other hand Ca^{2+}, which is a known inhibitor of RNase III activity (49,63), similarly blocked reactivity of *Sm*YbeY on dsRNA and generic structured RNA but did not compromise ssRNA cleavage. It is therefore tempting to speculate on Ca^{2+} and Mg^{2+}/Mn^{2+} availability as major environmental determinants of substrate selectivity and post-translational modulation of *Sm*YbeY activity *in vivo*. In this regard, it is worthy to note that the alteration of Mn^{2+} homeostasis sensitizes both bacterial intracellular pathogens and plant endosymbionts to the oxidative burst induced in the host during infection (64–66). *Sm*YbeY was able to degrade very efficiently the *in vitro* transcribed *ybeY* mRNA and therefore we cannot exclude the possibility of its autoregulation *in vivo*. Some RNases such as RNase E, RNase III and PNPase are also regulated at the post-transcriptional level by feedback loops involving decay of their own mRNA (61). This hypothesis of *Sm*YbeY autoregulation should be similarly explored in the future.

*Sm*YbeY activity influences fundamental and symbiotic functions

Absence or depletion of YbeY in bacteria decreases growth rate, alters rRNA/ribosome profiles, enhances cell sensitivity to stress and affects virulence and symbiotic traits (7,8,10,13–15,27,28). To explore the molecular basis of this pleiotropic phenotype in *S. meliloti* we profiled the *Sm*YbeY-dependent transcriptome on oligonucleotide-based microarrays. Contrary to the expected effect of the removal of an endoribonuclease on the RNA steady-state levels, down-regulated transcripts far outnumbered up-regulated transcripts in the *S. meliloti* YbeY mutant. However, this has been a common finding of similar studies addressing the influence of the activity of diverse endo and exoribonucleases in the bacterial transcriptome, including the *E. coli* and *Thermus thermophilus* YbeY orthologs, particularly upon stress exposure (27,67–70). Down-regulated genes could be mostly regarded as secondary molecular targets of *Sm*YbeY whose expression is positively influenced by this RNase in an indirect manner, e.g. involving alteration of regulatory intermediates or other yet unknown mechanisms. Nonetheless, a handful of *Sm*YbeY-bound mRNAs identified in our CoIP experiments were also found among this group of down-regulated transcripts. This finding suggests a direct interaction of *Sm*YbeY with these mRNAs in a protective mode that remains to be explored. Such a minor residual protective role in the stabilization of dsRNA and sRNAs has been already proposed for the long considered strictly catalytic ribonucleases RNase III and PNPase, respectively (61,71,72). Genes positively influenced by *Sm*YbeY included those encoding relevant protein components of energy producing pathways, a number of RNases (e.g. PNPase, RNase III or RNase D) and key

elements of the translation machinery. It is well-known that down-regulation of these fundamental physiological functions severely compromises bacterial growth and recovery upon stress exposure.

Protein mistranslation has been reported in *E. coli* YbeY mutants and was mainly attributed to the involvement of YbeY in rRNA maturation and ribosome quality control (5,13–16). Indeed, misprocessing of the 16S rRNA is a major molecular phenotype linked to YbeY loss-of-function in several bacterial species (5,7,8,13). In contrast, our results did not evidence an obvious involvement of *Sm*YbeY in rRNA maturation. This was an unexpected finding since it has been shown that a number of bacterial YbeY orthologs can indistinctly rescue the pleiotropic physiological phenotypes of different Δ*ybeY* mutants (5). The differences in substrate specificity and probably in activity mechanisms highlighted above may explain this apparent discrepancy. However, rRNA maturation involves the concerted activity of a suite of RNases some of which are not essential, can exhibit functional overlap or are interchangeable (61,67,68). Large genomes such as that of *S. meliloti* are typical sources of genetic redundancy that confers robustness to fundamental physiological processes (31). Therefore, we cannot rule out a role of *Sm*YbeY in rRNA maturation that may be efficiently complemented by functionally related RNases.

Our transcriptomic analyses evidenced that *Sm*YbeY influenced on chromosomal and pSymA-encoded functions to a similar extent. *S. meliloti* pSymA is a megaplasmid of mosaic origin that mostly host accessory acquired genes that specify relevant strain-specific and symbiotic traits (31). Major late symbiotic functions are coordinated via the two-component regulatory system FixLJ and the master regulators of nitrogen fixation NifA and FixK under microoxic conditions within the root nodule (73). Notably, we found that the *nifA* and *fixK* genes and a number of FixK-dependent gene clusters encoding the microaerobic denitrification pathway and elements of the electron transport chain associated with the nitrogenase complex were up-regulated in the *Sm*YbeY mutant, particularly during exponential growth. Interestingly, YbeY has been also shown to severely disturb regulation of the *Yersinia* virulence plasmid pYV (7). These independent findings hint at a major universal role of YbeY in the post-transcriptional control of prokaryotic gene networks relevant to the interaction with eukaryotic hosts.

Extensive comparison of the Hfq and *Sm*YbeY post-transcriptional regulons revealed a discrete overlap between the arrays of molecular targets of the two proteins. However, a number of known Hfq-binding mRNAs (26) exhibited accumulation patterns in the Hfq and *Sm*YbeY defective mutants compatible with a role of this RNase in the decay of these transcripts. It has been reported that Hfq actively competes for binding to the sites of the major endoribonuclease RNase E (typically AU-rich regions) within sRNAs and mRNAs, thereby protecting these transcripts from RNase E cleavage and further exoribonucleolytic degradation (74,75). Our results revealed that sets of mRNAs with increased steady-state levels in the Sm*ΔybeY* mutant are encoded by genes positively regulated by Hfq, namely metabolic, carbohydrate transport, regulatory, flagellar, nitrogen-fixation and denitrification genes. Further supporting an Hfq-mediated stabilization, these mRNAs have been shown to be mostly recovered in their entire length by pull down with Hfq (26). Therefore, it can be hypothesized that *Sm*YbeY has a role in the silencing of non-functional transcriptional output of flagellar and oxygen-regulated FixLJ-dependent mRNAs during stationary growth and under free-living non-symbiotic conditions, respectively (76,77).

*Sm*YbeY mediates silencing of sRNA-regulated mRNAs

Ribonucleases are also key active players at different levels in the post-transcriptional gene silencing mediated by antisense and *trans*-acting sRNAs (78). RNase E and PNPase are known to affect sRNA turnover whereas RNase III can be recruited to the sRNA-target mRNA interplay for the cleavage of the double-stranded RNA duplex with the consequent degradation of the message in a mechanism that resembles eukaryotic RNA interference (43,78,79). We have shown that *Sm*YbeY efficiently cleaves dsRNA and that asRNA–mRNA duplexes were remarkably abundant in CoIP–RNA. Thus, *Sm*YbeY-mediated silencing of some Hfq-protected mRNAs can be triggered by antisense interaction with asRNAs. In this regard, recent RNAseq-based surveys of the *S. meliloti* transcriptome have uncovered functionally significant pervasive antisense transcription of pSymA-borne symbiotic genes (39,40,80). Therefore, the involvement of *Sm*YbeY in the asRNA-mediated decay of nitrogen fixation mRNAs is a plausible scenario that merits further investigation.

RNase E has been already shown to be required for *trans*-sRNA regulation of cell-cycle and quorum-sensing mRNAs in *S. meliloti* (48,81). In contrast to what has been described for *E. coli* (27), transcriptomics data uncovered a scarce influence of *Sm*YbeY on the steady-state levels of *trans*-sRNAs. However, among the transcripts up-regulated in the *Sm*YbeY mutant we found a number of mRNAs coding for amino acid transporters that are putative targets of the Hfq-dependent homologous α-proteobacterial AbcR1 and AbcR2 sRNAs (37,54,82–84). Co-IP with Hfq typically recovers a specific stretch of these mRNAs, mostly derived from their 5′ regions, rather than the full-length transcripts (26). This likely indicates that these mRNAs undergo ribonucleolytic degradation upon antisense interaction with their sRNA partners at sites within the stretch bound by Hfq. We have tested this hypothesis with the proline betaine *prbA* mRNA, which is an experimentally confirmed target of both AbcR1 and AbcR2 *trans*-sRNAs (26). Fluorescence of relevant reporter strains along with *in vitro* assays suggested that post-transcriptional silencing of *prbA* could be initiated by *Sm*YbeY-mediated cleavage of the message at discrete positions upon AbcR2 interaction in the vicinity of the ribosome binding site. Previous works in *S. meliloti*, *E. coli* and *V. cholerae* had anticipated a major role of YbeY in riboregulation (8,10,27). However, this conclusion was entirely based on the misregulation of sets of sRNAs and their predicted mRNA targets upon deletion or depletion of YbeY, which does not demonstrate a direct role of this protein, either protective or catalytic, in the establishment of specific experimentally probed sRNA–mRNA interactions.

Therefore, our results add *Sm*YbeY to the repertoire of bacterial ribonucleases involved in RNA-mediated silencing.

In summary, we have shown that the highly conserved *S. meliloti* YbeY protein is a versatile metal-dependent double and single-strand endoribonuclease that influences turnover of bulk and sRNA-regulated mRNAs. The *Sm*YbeY-dependent mRNA network presented here provides a solid resource for the forthcoming investigation of *Sm*YbeY activity mechanisms underlying the post-transcriptional regulation of core RNA metabolism, energy producing pathways and late symbiotic functions in *S. meliloti*.

SUPPLEMENTARY DATA

Supplementary Data are available at NAR Online.

ACKNOWLEDGEMENTS

The authors thank Omar Torres-Quesada for early genetic constructs to generate the YbeY mutant, Vicenta Millán and Teresa Baptista da Silva for their invaluable technical assistance, Andreas Kautz for help in the transcriptome experiments, Jochen Blom and Oliver Rupp for bioinformatics services, Bernadette Boomers for genome sequencing, and the core facilities of EEZ-CSIC for routine sequencing of plasmid inserts.

FUNDING

Ministerio de Economía y Competitividad [ERDF-cofinanced grant BFU2013-48282-C2-2-P to J.I.J.-Z.]; LOEWE Program of the State of Hesse [SYNMIKRO to A.B]; German Research Foundation [CRC 987 to A.B.]; Fundação para a Ciência e Tecnologia (FCT) [Project LISBOA-01-0145-FEDER-007660 (Microbiologia Molecular, Estrutural e Celular - R&D Unit, UID/CBQ/04612/2013) funded by FEDER funds through COMPETE2020 - Programa Operacional Competitividade e Internacionalização (POCI) and by national funds to C.M.A.]; FCT [project PTDC/BIA-MIC/1399/2014 to C.M.A]; European Union's Horizon 2020 Research and Innovation Programme [grant agreement no. 635536 to C.M.A.]; Consejo Superior de Investigaciones Científicas (CSIC) [JAEDoc Program contract to A.P.]; FCT Post-Doctoral Fellowships [SFRH/BPD/109464/2015 to M.S., SFRH/BPD/75887/2011 to R.G.M.]; Ministerio de Economía y Competitividad [Program of Formación Post-doctoral contract to M.R.]; BMBF [FKZ 031A533 within the de.NBI network]. Funding for open access charge: Ministerio de Economía y Competitividad.
Conflict of interest statement. None declared.

REFERENCES

1. Gil,R., Silva,F.J., Peretó,J. and Moya,A. (2004) Determination of the core of a minimal bacterial gene set. *Microbiol. Mol. Biol. Rev.*, **68**, 518–537.
2. Finn,R.D., Bateman,A., Clements,J., Coggill,P., Eberhardt,R.Y., Eddy,S.R., Heger,A., Hetherington,K., Holm,L., Mistry,J. *et al.* (2014) Pfam: the protein families database. *Nucleic Acids Res.*, **42**, D222–D230.
3. Davies,B.W. and Walker,G.C. (2008) A highly conserved protein of unknown function is required by *Sinorhizobium meliloti* for symbiosis and environmental stress protection. *J. Bacteriol.*, **190**, 1118–1123.
4. Akerley,B.J., Rubin,E.J., Novick,V.L., Amaya,K., Judson,N. and Mekalanos,J.J. (2002) A genome-scale analysis for identification of genes required for growth or survival of *Haemophilus influenzae*. *Proc. Natl. Acad. Sci. U.S.A.*, **99**, 966–971.
5. Davies,B.W., Köhrer,C., Jacob,A.I., Simmons,L.A., Zhu,J., Aleman,L.M., RajBhandary,U.L. and Walker,G.C. (2010) Role of *Escherichia coli* YbeY, a highly conserved protein, in rRNA processing. *Mol. Microbiol.*, **78**, 506–518.
6. Kobayashi,K., Ehrlich,S.D., Albertini,A., Amati,G., Andersen,K.K., Arnaud,M., Asai,K., Ashikaga,S., Aymerich,S., Bessieres,P. *et al.* (2003) Essential *Bacillus subtilis* genes. *Proc. Natl. Acad. Sci. U.S.A*, **100**, 4678–4683.
7. Leskinen,K., Varjosalo,M. and Skurnik,M. (2015) Absence of YbeY RNase compromises the growth and enhances the virulence plasmid gene expression of *Yersinia enterocolitica* O:3. *Microbiology*, **161**, 285–299.
8. Vercruysse,M., Köhrer,C., Davies,B.W., Arnold,M.F.F., Mekalanos,J.J., RajBhandary,U.L. and Walker,G.C. (2014) The highly conserved bacterial RNase YbeY is essential in *Vibrio cholerae*, playing a critical role in virulence, stress regulation, and RNA processing. *PLoS Pathog.*, **10**, e1004175.
9. Oganesyan,V., Busso,D., Brandsen,J., Chen,S., Jancarik,J., Kim,R. and Kim,S.-H. (2003) Structure of the hypothetical protein AQ_1354 from *Aquifex aeolicus*. *Acta Crystallogr. D Biol. Crystallogr.*, **59**, 1219–1223.
10. Pandey,S.P., Minesinger,B.K., Kumar,J. and Walker,G.C. (2011) A highly conserved protein of unknown function in *Sinorhizobium meliloti* affects sRNA regulation similar to Hfq. *Nucleic Acids Res.*, **39**, 4691–4708.
11. Tatusov,R.L., Fedorova,N.D., Jackson,J.D., Jacobs,A.R., Kiryutin,B., Koonin,E.V., Krylov,D.M., Mazumder,R., Mekhedov,S.L., Nikolskaya,A.N. *et al.* (2003) The COG database: an updated version includes eukaryotes. *BMC Bioinformatics*, **4**, 41.
12. Zhan,C., Fedorov,E.V., Shi,W., Ramagopal,U.A., Thirumuruhan,R., Manjasetty,B.A., Almo,S.C., Fiser,A., Chance,M.R. and Fedorov,A.A. (2005) The YbeY protein from *Escherichia coli* is a metalloprotein. *Acta Crystallogr. Sect. F Struct. Biol. Cryst. Commun.*, **61**, 959–963.
13. Jacob,A.I., Köhrer,C., Davies,B.W., RajBhandary,U.L. and Walker,G.C. (2013) Conserved bacterial RNase YbeY plays key roles in 70S ribosome quality control and 16S rRNA maturation. *Mol. Cell*, **49**, 427–438.
14. Rasouly,A., Davidovich,C. and Ron,E.Z. (2010) The heat shock protein YbeY is required for optimal activity of the 30S ribosomal subunit. *J. Bacteriol.*, **192**, 4592–4596.
15. Rasouly,A., Schonbrun,M., Shenhar,Y. and Ron,E.Z. (2009) YbeY, a heat shock protein involved in translation in *Escherichia coli*. *J. Bacteriol.*, **191**, 2649–2655.
16. Grinwald,M. and Ron,E.Z. (2013) The *Escherichia coli* translation-associated heat shock protein YbeY is involved in rRNA transcription antitermination. *PLoS One*, **8**, e62297.
17. Sulthana,S., Basturea,G.N. and Deutscher,M.P. (2016) Elucidation of pathways of ribosomal RNA degradation: an essential role for RNase E. *RNA*, **22**, 1163–1171.
18. Boland,A., Tritschler,F., Heimstädt,S., Izaurralde,E. and Weichenrieder,O. (2010) Crystal structure and ligand binding of the MID domain of a eukaryotic Argonaute protein. *EMBO Rep.*, **11**, 522–527.
19. Parker,J.S., Parizotto,E.A., Wang,M., Roe,S.M. and Barford,D. (2009) Enhancement of the seed-target recognition step in RNA silencing by a PIWI/MID domain protein. *Mol. Cell*, **33**, 204–214.
20. Storz,G., Vogel,J. and Wassarman,K.M. (2011) Regulation by small RNAs in bacteria: expanding frontiers. *Mol. Cell*, **43**, 880–891.
21. Vogel,J. and Luisi,B.F. (2011) Hfq and its constellation of RNA. *Nat. Rev. Microbiol.*, **9**, 578–589.
22. Sobrero,P. and Valverde,C. (2012) The bacterial protein Hfq: much more than a mere RNA-binding factor. *Crit. Rev. Microbiol.*, **38**, 276–299.
23. Romby,P. and Charpentier,E. (2010) An overview of RNAs with regulatory functions in gram-positive bacteria. *Cell Mol. Life Sci.*, **67**, 217–237.
24. Sun,X., Zhulin,I. and Wartell,R.M. (2002) Predicted structure and phyletic distribution of the RNA-binding protein Hfq. *Nucleic Acids Res.*, **30**, 3662–3671.

25. Bardill,J.P. and Hammer,B. (2012) Non-coding sRNAs regulate virulence in the bacterial pathogen *Vibrio cholerae*. *RNA Biol.*, **9**, 392–401.
26. Torres-Quesada,O., Reinkensmeier,J., Schlueter,J.-P., Robledo,M., Peregrina,A., Giegerich,R., Toro,N., Becker,A. and Jimenez-Zurdo,J.I. (2014) Genome-wide profiling of Hfq-binding RNAs uncovers extensive post-transcriptional rewiring of major stress response and symbiotic regulons in *Sinorhizobium meliloti*. *RNA Biol.*, **11**, 563–579.
27. Pandey,S.P., Winkler,J.A., Li,H., Camacho,D.M., Collins,J.J. and Walker,G.C. (2014) Central role for RNase YbeY in Hfq-dependent and Hfq-independent small-RNA regulation in bacteria. *BMC Genomics*, **15**, 121.
28. Davies,B.W. and Walker,G.C. (2007) Identification of novel *Sinorhizobium meliloti* mutants compromised for oxidative stress protection and symbiosis. *J. Bacteriol.*, **189**, 2110–2113.
29. Beringer,J.E. (1974) R factor transfer in *Rhizobium leguminosarum*. *J. Gen. Microbiol.*, **84**, 188–198.
30. Robertsen,B.K., Aman,P., Darvill,A.G., McNeil,M. and Albersheim,P. (1981) Host-symbiont interactions: V. the structure of acidic extracellular polysaccharides secreted by *Rhizobium leguminosarum* and *Rhizobium trifolii*. *Plant Physiol.*, **67**, 389–400.
31. Galibert,F., Finan,T.M., Long,S.R., Puhler,A., Abola,P., Ampe,F., Barloy-Hubler,F., Barnett,M.J., Becker,A., Boistard,P. *et al.* (2001) The composite genome of the legume symbiont *Sinorhizobium meliloti*. *Science*, **293**, 668–672.
32. Bahlawane,C., McIntosh,M., Krol,E. and Becker,A. (2008) *Sinorhizobium meliloti* regulator MucR couples exopolysaccharide synthesis and motility. *Mol. Plant Microbe Interact.*, **21**, 1498–1509.
33. Schafer,A., Tauch,A., Jager,W., Kalinowski,J., Thierbach,G. and Puhler,A. (1994) Small mobilizable multi-purpose cloning vectors derived from the *Escherichia coli* plasmids pK18 and pK19: selection of defined deletions in the chromosome of *Corynebacterium glutamicum*. *Gene*, **145**, 69–73.
34. Simon,R., Priefer,U. and Puhler,A. (1983) A broad host range mobilization system for in vivo genetic engineering: transposon mutagenesis in gram negative bacteria. *Nat. Biotech.*, **1**, 784–791.
35. Torres-Quesada,O., Oruezabal,R.I., Peregrina,A., Jofre,E., Lloret,J., Rivilla,R., Toro,N. and Jimenez-Zurdo,J.I. (2010) The *Sinorhizobium meliloti* RNA chaperone Hfq influences central carbon metabolism and the symbiotic interaction with alfalfa. *BMC Microbiol.*, **10**, 71.
36. Blatny,J.M., Brautaset,T., Winther-Larsen,H.C., Haugan,K. and Valla,S. (1997) Construction and use of a versatile set of broad-host-range cloning and expression vectors based on the RK2 replicon. *Appl. Environ. Microbiol.*, **63**, 370–379.
37. Torres-Quesada,O., Millán,V., Nisa-Martínez,R., Bardou,F., Crespi,M., Toro,N. and Jiménez-Zurdo,J.I. (2013) Independent activity of the homologous small regulatory RNAs AbcR1 and AbcR2 in the legume symbiont *Sinorhizobium meliloti*. *PLoS One*, **8**, e68147.
38. Langmead,B. and Salzberg,S.L. (2012) Fast gapped-read alignment with Bowtie 2. *Nat. Methods*, **9**, 357–359.
39. Schlüter,J.P., Reinkensmeier,J., Daschkey,S., Evguenieva-Hackenberg,E., Janssen,S., Janicke,S., Becker,J.D., Giegerich,R. and Becker,A. (2010) A genome-wide survey of sRNAs in the symbiotic nitrogen-fixing alpha-proteobacterium *Sinorhizobium meliloti*. *BMC Genomics*, **11**, 245.
40. Schlüter,J.P., Reinkensmeier,J., Barnett,M.J., Lang,C., Krol,E., Giegerich,R., Long,S.R. and Becker,A. (2013) Global mapping of transcription start sites and promoter motifs in the symbiotic alpha-proteobacterium *Sinorhizobium meliloti* 1021. *BMC Genomics*, **14**, 156.
41. Hilker,R., Stadermann,K.B., Doppmeier,D., Kalinowski,J., Stoye,J., Straube,J., Winnebald,J. and Goesmann,A. (2014) ReadXplorer—visualization and analysis of mapped sequences. *Bioinformatics*, **30**, 2247–2254.
42. Love,M.I., Huber,W. and Anders,S. (2014) Moderated estimation of fold change and dispersion for RNA-seq data with DESeq2. *Genome Biol.*, **15**, 550.
43. Viegas,S.C., Silva,I.J., Saramago,M., Domingues,S. and Arraiano,C.M. (2010) Regulation of the small regulatory RNA MicA by ribonuclease III: a target-dependent pathway. *Nucleic Acids Res.*, **39**, 2918–2930.
44. Milligan,J.F., Groebe,D.R., Witherell,G.W. and Uhlenbeck,O.C. (1987) Oligoribonucleotide synthesis using T7 RNA polymerase and synthetic DNA templates. *Nucleic Acids Res.*, **15**, 8783–8798.
45. Serrania,J., Vorhölter,F.-J., Niehaus,K., Pühler,A. and Becker,A. (2008) Identification of *Xanthomonas campestris* pv. campestris galactose utilization genes from transcriptome data. *J. Biotechnol.*, **135**, 309–317.
46. Becker,A., Barnett,M.J., Capela,D., Dondrup,M., Kamp,P.B., Krol,E., Linke,B., Ruberg,S., Runte,K., Schroeder,B.K. *et al.* (2009) A portal for rhizobial genomes: RhizoGATE integrates a *Sinorhizobium meliloti* genome annotation update with postgenome data. *J. Biotechnol.*, **140**, 45–50.
47. Dondrup,M., Albaum,S.P., Griebel,T., Henckel,K., Jünemann,S., Kahlke,T., Kleindt,C.K., Küster,H., Linke,B., Mertens,D. *et al.* (2009) EMMA 2 – A MAGE-compliant system for the collaborative analysis and integration of microarray data. *BMC Bioinformatics*, **10**, 50–50.
48. Robledo,M., Frage,B., Wright,P.R. and Becker,A. (2015) A stress-induced small RNA modulates alpha-rhizobial cell cycle progression. *PLoS Genet.*, **11**, e1005153.
49. Li,H.L., Chelladurai,B.S., Zhang,K. and Nicholson,A.W. (1993) Ribonuclease III cleavage of a bacteriophage T7 processing signal. Divalent cation specificity, and specific anion effects. *Nucleic Acids Res.*, **21**, 1919–1925.
50. Gross,G. and Dunn,J.J. (1987) Structure of secondary cleavage sites of *E. coli* RNAaseIII in A3t RNA from bacteriophage T7. *Nucleic Acids Res.*, **15**, 431–442.
51. Nicholson,A.W. (2014) Ribonuclease III mechanisms of double-stranded RNA cleavage. *Wiley Interdiscip. Rev. RNA*, **5**, 31–48.
52. Barra-Bily,L., Fontenelle,C., Jan,G., Flechard,M., Trautwetter,A., Pandey,S.P., Walker,G.C. and Blanco,C. (2010) Proteomic alterations explain phenotypic changes in *Sinorhizobium meliloti* lacking the RNA chaperone Hfq. *J. Bacteriol.*, **192**, 1719–1729.
53. Gao,M., Barnett,M.J., Long,S.R. and Teplitski,M. (2010) Role of the *Sinorhizobium meliloti* global regulator Hfq in gene regulation and symbiosis. *Mol. Plant Microbe Interact.*, **23**, 355–365.
54. Sobrero,P., Schluter,J.P., Lanner,U., Schlosser,A., Becker,A. and Valverde,C. (2012) Quantitative proteomic analysis of the Hfq-regulon in *Sinorhizobium meliloti* 2011. *PLoS One*, **7**, e48494.
55. Sittka,A., Lucchini,S., Papenfort,K., Sharma,C.M., Rolle,K., Binnewies,T.T., Hinton,J.C.D. and Vogel,J. (2008) Deep sequencing analysis of small noncoding RNA and mRNA targets of the global post-transcriptional regulator, Hfq. *PLoS Genet.*, **4**, e1000163.
56. Sittka,A., Sharma,C.M., Rolle,K. and Vogel,J. (2009) Deep sequencing of *Salmonella* RNA associated with heterologous Hfq proteins in vivo reveals small RNAs as a major target class and identifies RNA processing phenotypes. *RNA Biol.*, **6**, 266–275.
57. Berghoff,B.A., Glaeser,J., Sharma,C.M., Zobawa,M., Lottspeich,F., Vogel,J. and Klug,G. (2011) Contribution of Hfq to photooxidative stress resistance and global regulation in *Rhodobacter sphaeroides*. *Mol. Microbiol.*, **80**, 1479–1495.
58. Dambach,M., Irnov,I. and Winkler,W.C. (2013) Association of RNAs with *Bacillus subtilis* Hfq. *PLoS One*, **8**, e55156.
59. Chao,Y., Papenfort,K., Reinhardt,R., Sharma,C.M. and Vogel,J. (2012) An atlas of Hfq-bound transcripts reveals 3′ UTRs as a genomic reservoir of regulatory small RNAs. *EMBO J.*, **31**, 4005–4019.
60. Saadeh,B., Caswell,C.C., Chao,Y., Berta,P., Wattam,A.R., Roop,R.M. and O'Callaghan,D. (2016) Transcriptome-wide Identification of Hfq-associated RNAs in *Brucella suis* by deep sequencing. *J. Bacteriol.*, **198**, 427–435.
61. Arraiano,C.M., Andrade,J.M., Domingues,S., Guinote,I.B., Malecki,M., Matos,R.G., Moreira,R.N., Pobre,V., Reis,F.P., Saramago,M. *et al.* (2010) The critical role of RNA processing and degradation in the control of gene expression. *FEMS Microbiol. Rev.*, **34**, 883–923.
62. Kaberdin,V.R., Walsh,A.P., Jakobsen,T., McDowall,K.J. and von Gabain,A. (2000) Enhanced cleavage of RNA mediated by an interaction between substrates and the arginine-rich domain of *E. coli* ribonuclease E1. *J. Mol. Biol.*, **301**, 257–264.
63. Li,H. and Nicholson,A.W. (1996) Defining the enzyme binding domain of a ribonuclease III processing signal. Ethylation

interference and hydroxyl radical footprinting using catalytically inactive RNase III mutants. *EMBO J.*, **15**, 1421–1433.
64. Davies,B.W. and Walker,G.C. (2007) Disruption of *sitA* Compromises *Sinorhizobium meliloti* for manganese uptake required for protection against oxidative stress. *J. Bacteriol.*, **189**, 2101–2109.
65. Papp-Wallace,K.M. and Maguire,M.E. (2006) Manganese transport and the role of manganese in virulence. *Ann. Rev. Microbiol.*, **60**, 187–209.
66. Anderson,E.S., Paulley,J.T., Gaines,J.M., Valderas,M.W., Martin,D.W., Menscher,E., Brown,T.D., Burns,C.S. and Roop,R.M. (2009) The manganese transporter MntH is a critical virulence determinant for *Brucella abortus* 2308 in experimentally infected mice. *Infect. Immun.*, **77**, 3466–3474.
67. Pobre,V. and Arraiano,C.M. (2015) Next generation sequencing analysis reveals that the ribonucleases RNase II, RNase R and PNPase affect bacterial motility and biofilm formation in *E. coli*. *BMC Genomics*, **16**, 72.
68. Stead,M.B., Marshburn,S., Mohanty,B.K., Mitra,J., Castillo,L.P., Ray,D., van Bakel,H., Hughes,T.R. and Kushner,S.R. (2011) Analysis of *Escherichia coli* RNase E and RNase III activity in vivo using tiling microarrays. *Nucleic Acids Res.*, **39**, 3188–3203.
69. Mohanty,B.K. and Kushner,S.R. (2003) Genomic analysis in *Escherichia coli* demonstrates differential roles for polynucleotide phosphorylase and RNase II in mRNA abundance and decay. *Mol. Microbiol.*, **50**, 645–658.
70. Ohyama,H., Sakai,T., Agari,Y., Fukui,K., Nakagawa,N., Shinkai,A., Masui,R. and Kuramitsu,S. (2014) The role of ribonucleases in regulating global mRNA levels in the model organism *Thermus thermophilus* HB8. *BMC Genomics*, **15**, 386–386.
71. Bandyra,K.J., Sinha,D., Syrjanen,J., Luisi,B.F. and De Lay,N.R. (2016) The ribonuclease polynucleotide phosphorylase can interact with small regulatory RNAs in both protective and degradative modes. *RNA*, **22**, 360–372.
72. Gan,J., Tropea,J.E., Austin,B.P., Court,D.L., Waugh,D.S. and Ji,X. (2006) Structural insight into the mechanism of double-stranded RNA processing by ribonuclease III. *Cell*, **124**, 355–366.
73. Bobik,C., Meilhoc,E. and Batut,J. (2006) FixJ: a major regulator of the oxygen limitation response and late symbiotic functions of *Sinorhizobium meliloti*. *J. Bacteriol.*, **188**, 4890–4902.
74. Folichon,M., Allemand,F., Regnier,P. and Hajnsdorf,E. (2005) Stimulation of poly(A) synthesis by *Escherichia coli* poly(A)polymerase I is correlated with Hfq binding to poly(A) tails. *FEBS J.*, **272**, 454–463.
75. Moll,I., Afonyushkin,T., Vytvytska,O., Kaberdin,V.R. and Blasi,U. (2003) Coincident Hfq binding and RNase E cleavage sites on mRNA and small regulatory RNAs. *RNA*, **9**, 1308–1314.
76. Sourjik,V., Muschler,P., Scharf,B. and Schmitt,R. (2000) VisN and VisR are global regulators of chemotaxis, flagellar, and motility genes in *Sinorhizobium (Rhizobium) meliloti*. *J. Bacteriol.*, **182**, 782–788.
77. Rotter,C., Mühlbacher,S., Salamon,D., Schmitt,R. and Scharf,B. (2006) Rem, a new transcriptional activator of motility and chemotaxis in *Sinorhizobium meliloti*. *J. Bacteriol.*, **188**, 6932–6942.
78. Saramago,M., Bárria,C., dos Santos,R.F., Silva,I.J., Pobre,V., Domingues,S., Andrade,J.M., Viegas,S.C. and Arraiano,C.M. (2014) The role of RNases in the regulation of small RNAs. *Curr. Opin. Microbiol.*, **18**, 105–115.
79. Andrade,J.M., Pobre,V., Matos,A.M. and Arraiano,C.M. (2012) The crucial role of PNPase in the degradation of small RNAs that are not associated with Hfq. *RNA*, **18**, 844–855.
80. Robledo,M., Jiménez-Zurdo,J.I. and Becker,A. (2015) Antisense transcription of symbiotic genes in *Sinorhizobium meliloti*. *Symbiosis*, **67**, 55–67.
81. Baumgardt,K., Šmídová,K., Rahn,H., Lochnit,G., Robledo,M. and Evguenieva-Hackenberg,E. (2015) The stress-related, rhizobial small RNA RcsR1 destabilizes the autoinducer synthase encoding mRNA *sinI* in *Sinorhizobium meliloti*. *RNA Biol.*, **13**, 486–499.
82. Wilms,I., Voss,B., Hess,W.R., Leichert,L.I. and Narberhaus,F. (2011) Small RNA-mediated control of the *Agrobacterium tumefaciens* GABA binding protein. *Mol. Microbiol.*, **80**, 492–506.
83. Caswell,C.C., Gaines,J.M., Ciborowski,P., Smith,D., Borchers,C.H., Roux,C.M., Sayood,K., Dunman,P.M. and Roop Ii,R.M. (2012) Identification of two small regulatory RNAs linked to virulence in *Brucella abortus* 2308. *Mol. Microbiol.*, **85**, 345–360.
84. Overlöper,A., Kraus,A., Gurski,R., Wright,P.R., Georg,J., Hess,W.R. and Narberhaus,F. (2014) Two separate modules of the conserved regulatory RNA AbcR1 address multiple target mRNAs in and outside of the translation initiation region. *RNA Biol.*, **11**, 624–640.